Synthetic Peptide Drugs for Targeting Skin Cancer: Malignant Melanoma and Melanotic Lesions

Alex N. Eberle[1,2*], Bhimsen Rout[3], Mei Bigliardi-Qi[3] and Paul L. Bigliardi[3,4*]

[1]Department of Biomedicine, University of Basel, Switzerland
[2]Collegium Helveticum, ETH Zurich, Switzerland
[3]Institute of Medical Biology, A*STAR, Biopolis, Singapore
[4]YLL School of Medicine, National University of Singapore NUS and University Medicine Clinic, National University Hospital NUHS, Singapore

Abstract

Background: Peptides play decisive roles in the skin, ranging from host defense responses to various forms of neuroendocrine regulation of cell and organelle function. Synthetic peptides conjugated to radionuclides or photosensitizers may serve to identify and treat skin tumors and their metastatic forms in other organs of the body. In the introductory part of his review, the role and interplay of the different peptides in the skin is briefly summarized, including their potential application for the management of frequently occurring skin cancers. Special emphasis is given to different targeting options for the treatment of melanoma and melanotic lesions.
Radionuclide targeting: α-Melanocyte-stimulating hormone (α-MSH) is the most prominent peptide for targeting of melanoma tumors via the G protein-coupled melanocortin-1 receptor that is (over-)expressed by melanoma cells and melanocytes. More than 100 different linear and cyclic analogs of α-MSH containing chelators for ^{111}In, $^{67/68}$Ga, ^{64}Cu, ^{90}Y, ^{212}Pb, ^{99m}Tc, ^{188}Re were synthesized and examined with experimental animals and in a few clinical studies. Linear Ac-Nle-Asp-His-*D*-Phe-Arg-Trp-Gly-Lys-NH_2 (NAP-amide) and Re-cyclized Cys-Cys-Glu-His-*D*-Phe-Arg-Trp-Cys-Arg-Pro-Val-NH_2 (Re[Arg^{11}]CCMSH) containing different chelators at the N- or C-terminus served as lead compounds for peptide drugs with further optimized characteristics. Alternatively, melanoma may be targeted with radiopeptides that bind to melanin granules occurring extracellularly in these tumors.
Photosensitizer targeting: A more recent approach is the application of photosensitizers attached to the MSH molecule for targeted photodynamic therapy using LED or coherent laser light that specifically activates the photosensitizer. Experimental studies have demonstrated the feasibility of this approach as a more gentle and convenient alternative compared to radionuclides.

*Corresponding authors:
alex-n.eberle@unibas.ch
paul.bigliardi@gmail.com

Key Words:
Melanocyte-stimulating hormone (MSH); melanocortin-1 receptor (MC1R); radiometal; photosensitizer; malignant melanoma; metastasis; melanin-binding peptide; photodynamic therapy

Short title (if applicable):
Peptide targeting of melanoma

INTRODUCTION

The skin of all vertebrate species is the site of origin as well as the site of action of numerous biologically active peptides that show a broad spectrum of activities ranging from host defense responses to various forms of neuroendocrine regulation of cell and organelle function [1–4]. For example, of the more than 100 human antimicrobial peptides known, over a dozen have been shown to occur in the skin (e.g. β-defensins, dermcidin, drosomycin-like defensin, RNase 5 and 7, chemokines such as chemokine ligand 20, psoriasin, koebnerisin, chimerins). These peptides represent key components of the innate immune system, thus forming an integral part of the first line of defense [5–9]). Some of these host-defense peptides also have the potential to serve as anticancer agents in the skin [10]. Human skin has long been recognized as an endocrine organ producing several neuropeptides (e.g. α-melanotropin (α-MSH), adrenocorticotropin (ACTH), corticoliberin (CRH), endorphin, enkephalin, substance P, calcitonin gene-related peptide (CGRP), neuropeptide Y (NPY), vasointestinal peptide (VIP), somatostatin, bradykinin, endothelin, endogenous peptide) which participate in the regulation of skin function [1, 2, 11–20]. Some of these peptides may play a role in cancer therapy with cytotoxic agents or radioactivity, e.g. as vehicles for specific targeting of cancer cells in the skin [21]. Furthermore, several skin peptides from other species, in particular from frog skin, have been recognized to exhibit cytotoxicity against tumor cells [22]. Thus, there are a variety of peptides originating from skin that have the potential to be developed into antitumor agents for treatment of skin cancer.

The three main types of skin cancer include basal cell carcinoma (BCC) [23], squamous cell carcinoma (SCC) [24] and melanoma [25]. Other types of skin cancer or adnexal tumors, e.g. sweat gland and sebaceous gland carcinomas [26], non-melanoma nail neoplasms [27], keratoacanthoma [28], Merkel cell carcinoma (APUDoma) [29], are less common and treatment options are varying. Of the non-melanoma skin cancers, BCC is the most abundant (approx. 80%) with over 3.5 million new cases in the USA and Europe annually [23]; excessive exposure to sunlight is the major risk factor. BCC is derived from non-keratinizing cells of the basal layer of the epidermis, generally grows slowly and rarely metastasizes [30]. Current treatment options of BCC include standard excision, Mohs micrographic surgery, electrodesiccation and curettage, cryosurgery, radiation therapy, photodynamic therapy, 5-fluorouracil or imiquimod (an immune modifier) and for extensive cases hedgehog signaling pathway inhibitors such as vismodegib [31]. SCC accounts for about 20% of non-melanoma skin cancers and originates from squamous cells of the epidermis, typically forming slowly growing nodules which may ulcerate. The individual risk of SCC is associated to sun exposure in the last 10 years prior to diagnosis [32]. It is twice as prevalent in men as in women and unlike BCC, SCC has a substantial risk of metastasis. Treatment options of localized SCC are similar to those described for BCC; locally advanced and metastatic SCC may be cured successfully by chemotherapy (e.g. cisplatin, 5-fluorouracil), or targeting agents (e.g. cetuximab), with an overall response rate up to 70% [33]. Recently, cationic membrane active peptides have been studied preclinically for the treatment of SCC; melittin was the most promising in inhibiting growth of SCC cells and turned out to be more efficient than 5-fluorouracil [34]. Similarly, G protein-coupled receptor ligands such as galanin may play a role in inhibiting SCC proliferation: Activation of the galanin receptor type 1 inhibits cell growth via effects on the cell cycle, and activation of the galanin receptor type 2 reduces cell proliferation and enhances cell apoptosis [35].

Malignant melanoma is about 20 times less abundant than BCC and SCC but it is much more aggressive, showing a death rate of 2.3 to 2.7 per 100,000 persons in Europe and

the USA [36, 37]. Worldwide, about 232,000 new cases of melanoma were diagnosed and about 55,000 melanoma-related deaths occurred in 2012 [38]. The prevalence of melanoma is also associated with exposure to UV light: Large numbers of acquired melanocytic nevi, induced by sunburns in childhood, are a strong risk factor for the development of melanoma in adults [39]. Treatment of early-stage melanoma is definitively by surgery, accompanied by adjuvant interferon-α therapy for persons at risk of recurrence. Metastatic melanoma treated by chemotherapy (dacarbazine), interleukin 2 or combinations frequently yields modest results whereas more modern approaches such as cytotoxic T-lymphocyte-associated antigen 1 (CTLA-1) blocking antibodies (ipilimumab) or programmed cell death 1 receptor (PD-1) inhibiting antibodies (pembrolizumab, nivolumab) and combinations thereof appear to be more promising [40]. Surgery has received a prominent role again along with modern approaches of treatment of advanced melanoma [41]. Oncolytic viruses, e.g. imlygic (talimogene laherparepvec/T-Vec, a herpesvirus-based vector optimised for oncolytic and immunomodulatory activities) represent a new class of anti-melanoma agents that have recently been approved for treatment [42]. Currently, the highest survival rates are obtained for melanoma patients with the BRAF V600E mutation with vemurafenib, dabrafenib or trametinib that are low molecular weight inhibitors of the B-Raf serine-threonine kinase [43, 44]. In melanoma cells harboring the BRAF V600E mutations, the mitogen-activated protein kinase (MAPK) pathway is permanently activated, which ultimately leads to uncontrolled cell proliferation and which can be reversed by inhibition of B-Raf. However, even though 40% and more of the patients with advanced melanoma may initially respond to this treatment, the frequently observed development of resistance and development of SCCs and BRAF-negative melanomas 3–4 months into the treatment may prevent cure [45, 46]. New strategies combining B-Raf inhibitors with checkpoint inhibitor immunotherapy (CTLA-1 and PD-1 antibodies) may solve some of these problems.

In spite of the progress outlined above, treatment of advanced melanoma still remains an unresolved problem for many patients. The same is true for hypermelanotic or dysplastic lesions in areas where surgery is problematic or when large surface lesions are present in frail, elderly patients with contraindications for anesthesia or long operations. Peptides may fill some of the gaps although none of them has yet reached the stage of routine application in the clinic. Figure **1** shows the prominent role which peptides are playing in the complex network of therapeutic approaches for the management of melanoma and also of other types of skin cancer. Peptides serve important functions in the preclinical development of small molecules and antibodies but may be developed as drugs in their own right in the future.

This review will focus on the current state of research about radiolabeled peptides for peptide receptor radiation therapy (PRRT) or melanin-binding peptide radiation therapy (MPRT) of melanoma, and about phototoxic peptides for specific photodynamic therapy (PDT) of dysplastic lesions and melanoma. The first part will be devoted to radiopeptide analogs of α-melanocyte-stimulating hormone (α-melanotropin, α-MSH) for PRRT, the second part to melanin-binding radiopeptides (MBP) for MPRT, and the third part to MSH peptides containing photosensitizers for PDT.

PEPTIDE TARGETING OPTIONS FOR MELANOMA

α-MSH and its analogs are the most widely investigated group of peptides as targeting option for malignant melanoma. The main physiological role of α-MSH in the skin is to induce melanogenesis in melanocytes and melanoma cells and, in concert with other neuro-endocrine regulators, to control melanoblast migration and differentiation (reviewed in [12, 47, 48]). MSH peptides induce melanogenesis by interaction with the G protein-coupled melanocortin-1 receptor (MC1R) which was originally identified by binding studies on mouse and human melanoma cells [49–51] as well as by photoaffinity labeling [52–54]. MC1R was also the first member of the melanocortin receptor family (MC1R–MC5R) that had been cloned and sequenced [55, 56]. Whereas human melanocytes generally express low numbers of MC1R [57] and none of the other four MCR subtypes, melanoma cells frequently overexpress MC1R which is therefore regarded as a useful marker for malignant melanoma and an interesting target for radiolabeled peptides aimed at melanoma diagnosis and therapy [58–61]. MC1R is the target for, e.g., superpotent [Nle^4,*D*-Phe^7]-α-MSH (NDP-MSH) (melanotan I) [62, 63] or tetrapeptides and tripeptides containing the core sequence [64, 65] when hormone-induced tanning of the skin is envisaged, be it for cosmetic reasons or to protect the skin by an increased tan from the risk of melanoma formation. However, uncontrolled and prolonged use of potent MSH agonist peptides is risky on its own because of potential induction of malignant moles by the hormones [66]. In fact, a recent study demonstrated that chronic expression of agouti signaling peptide (ASIP), a physiological antagonist/inverse agonist of MC1R [67], in the tumor microenvironment of experimental cutaneous or metastatic lung melanoma provided a survival advantage to melanoma-bearing mice [68]. This demonstrates that persistent inhibition of MC1R may slow down melanoma tumor growth. And finally, the finding that MC1R germline variants confer risk for the development of BRAF-mutant melanoma (in the absence of UV light) shows that artificially induced tanning provides limited benefit or is even counterproductive [69].

Early attempts to develop MSH-based PRRT for the treatment of melanoma tumors date back to the 1970s when highly tritiated analogs of α-MSH were synthesized and later applied to *in vitro* and *in vivo* targeting experiments (reviewed in [47, 70]). The soft β^--radiation of tritium (~ 5.7 keV) was expected to minimize collateral damage in healthy tissue when radioactivity is accumulated in the tumor. However, studies with animal models showed that the radiotoxicity of these β^--particles was too low and the retention of the radionuclide by the tumor was too short to arrest melanoma cell growth *in vivo* [70]. On the other hand, these experiments demonstrated that radioactive peptides are readily taken up by tumor cells, mediated by internalization of the MC1R-ligand complex. In the early 1990s, analogs of α-MSH containing the diethylenetriaminepentaacetic acid (DTPA) chelator for incorporation of radiometals with high-energy emission were synthesized and tested for targeting of melanoma tumors in experimental animals [71–75]. This was the starting point for the study of a still growing number of currently worldwide >100 different radiolabeled α-MSH peptides containing various chelators and radiometals.

The principal lead peptides for melanoma targeting are summarized in Table 1. The natural sequence of α-MSH is not ideal for targeting purposes because the *in vitro* stability of α-MSH in human or rat plasma is insufficient and the half-life is short (20–40 min at 37°C) [47] and *in vivo* it is even shorter [76]. The Phe^7–Arg^8 bond of α-MSH is the primary cleavage site that leads to inactivation of the hormonal core sequence [62, 76]. This problem was resolved with the development of [Nle^4,*D*-Phe^7]-α-MSH (NDP-MSH)

that exhibits high metabolic stability [62] and formed the basis for the design of a number of similar MSH analogs and fragments (reviewed in [77, 78]). One of these is [Nle^4,Asp^5,*D*-Phe^7]-α-MSH$_{4-11}$ (NAP-amide) which proved to be very useful for targeting [79].

Apart from MC1R agonists, the antagonist/inverse agonist ASIP [67] and the physiologic antagonist β-defensin 3 (βD3) [80] have both been demonstrated to interact with MC1R. Whereas ASIP is a 131-residue peptide with a complex knot motif of five cystin bridges in the C-terminal part, βD3 is a 45-residue peptide with three cystins (reviewed in [81, 82]). Although the C-terminal ASIP$_{91-131}$ fragment displays full biologically activity [83], the minimal structures of ASIP and also of βD3 are too complicated for ready structure-activity studies necessary for developing an optimized targeting compound. The only short antagonist currently known for MC1R is a cyclic γ-MSH decapeptide (Table 1) that mimics the backbone structure of ASIP$_{117-122}$ thought to be essential for the interaction with MC1R [84]. Eventually, peptides for melanoma targeting based on this antagonist or on novel ASIP- or βD3-mimicking structures may become available in the future.

Another alternative for melanoma targeting are peptides that interact directly with melanin granules (Table 1). These melanin-binding peptides (MBP) were originally developed for studies of melanization by the fungus *Cryptococcus neoformans* during murine infection [85]. One of these peptides, 4B4, served as lead compound for the development of heptapeptides with a good potential for radiotargeting of melanoma [86]. MBP may replace an anti-melanin antibody previously used for radioimmunotherapy of melanoma [86]. A last peptide worth mentioning is the tyrosinase inhibitor decapeptide-12 which was shown to be effective in the treatment of melasma and lentigo [87]. The potential of decapeptide-12 for melanoma targeting has not yet been investigated but it is likely that the peptide is capable of penetrating cell and/or melanosome membranes.

RECEPTOR-MEDIATED TARGETING OF MELANOMA BY MSH RADIOPEPTIDES

Principles of radionuclide targeting of melanoma

The general principle of melanoma tumor targeting with MSH radiopeptides is outlined in Figure **2**. In most cases, radiolabeled MSH peptides are applied intravenously, leading to accumulation in the target organ and also in non-target tissues, mainly the kidneys, liver and spleen, but may also include bone marrow, intestines and skin. Binding of the radiopeptide to MC1R induces receptor down-regulation and internalization of the receptor-ligand complex [59, 88], the extent of which in humans may depend on the MC1R variant expressed [89]. GPCR receptor-ligand complexes are first found in endosomes (reviewed in [90]), and later, part of the radioactivity may accumulate in the nucleus and also in mitochondria [91]. The selection of the radioisotopes for MSH peptides depends on the purpose of the targeting: For diagnostic applications, isotopes emitting γ-radiation are necessary (e.g. ^{67}Ga, ^{99m}Tc, ^{111}In), or positron-emitters (e.g. ^{18}F, $^{62/64}$Cu, ^{68}Ga) which also produce γ-photons. For therapeutic application of MSH peptides, short-range α-emitters (e.g. ^{212}Pb) or high-energy β-emitters (e.g. ^{90}Y, ^{177}Lu, ^{67}Cu, ^{188}Re) are selected or, alternatively, isotopes that emit Auger electrons (e.g. ^{99m}Tc, ^{111}In). The insertion of radiometals into peptides requires suitable chelators [92] conjugated to the MSH peptides; selected chelators used in the context of melanoma targeting are presented below.

Before setting up any *in vivo* studies, the synthetic conjugates between MSH peptides and selected chelators are vigorously tested *in vitro*: A general scheme for radiopeptide development is found in [92]. The screening methods first applied for MSH peptides are receptor binding and bioassays using mouse and human melanoma cell lines for which K_D, K_i and/or IC_{50} values are determined. This is followed by a kinetic analysis of the cellular uptake of the radiopeptide and retention of the radionuclide by melanoma cells, an example of which is presented in Figure **3**. In addition, receptor autoradiography with melanoma tissue sections *in vitro* is frequently applied to examine MC1R distribution in the tumor [75]. *In vivo*, PET, planar scintigraphy or SPECT have become the primary examination methods, but autoradiography of tumor sections taken after *in vivo* biodistribution studies may complement imaging because it can unveil unconspicuous details of tumor lesions [79].

Chelators for radiometals used in melanoma targeting

As mentioned above, open-chain DTPA was the chelator employed for the initial studies of radiotargeting melanoma, not least because of the mild conditions for complex formation with ^{111}In [71-75]. However, the stability of DTPA-radiometal complexes *in vivo* was frequently insufficient, in particular that of [^{90}Y]DTPA [93]. On the other hand, the related (preorganized) cyclohexyl derivative of DTPA, *N*-(2-aminoethyl)-*trans*-1,2-diaminocyclohexane-*N,N′,N″*-pentaacetic acid (CHX-A-DTPA) [94] allowed for straightforward and efficient labeling of a cyclic MSH peptide with ^{68}Ga, ^{86}Y and ^{111}In [95]. Yet, despite the facile preparation of the different radioligands, tumor uptake and stability of these cyclic MSH analogs was moderate [95] and the application of this chelator was not pursued.

The development of the bifunctional cyclen 1,4,7,10-tetraazacyclododecane-1,4,7,10-tetraacetic acid (DOTA) [93] yielded a superior chelator for tumor targeting because the [radiometal]DOTA-peptide complexes are generally very stable *in vivo* (for detailed information, including chemical structures of many different chelators, see [92]). However, the disadvantage of DOTA is that complex formation with radiometals requires heat and takes up to one hour for completion which is a drawback for radionuclides with very short half-lives. An improved chelation method using microwave technology and requiring less than one minute has been introduced for the labeling of a cyclized DOTA-MSH analog [96]. Expansion of the 12-membered ring of DOTA to the 14-membered size of 4,11-*bis*(carboxymethyl)-1,4,8,11-tetraazabicyclo[6.6.2]hexadecane (CBTE2A) yields a cage that forms more stable complexes with ^{64}Cu than DOTA and thus higher specific radioactivity of the peptide can be obtained [97]. Reduction of the 12-membered ring of DOTA to the 9-membered ring of 1,4,7-triazacyclononane-1,4,7-triacetic acid (NOTA) results in an alternative chelator suitable for MSH peptides, as NOTA forms very stable complexes with $^{67/68}$Ga, ^{111}In and also ^{62}Cu under mild conditions and displays high conformational and size selectivity (see [92]). NOTA is more lipophilic than DOTA because of its neutral net charge when complexed with trivalent metal ions, leading to faster elimination through the kidneys. It has been conjugated to both cyclic and linear MSH peptides and complexed with ^{62}Cu and ^{64}Cu [98, 99].

Chelators for $(Tc{=}O)^{3+}$, $(Re{=}O)^{3+}$, $Tc(CO)_3^+$ and $Re(CO)_3^+$ cores and the different steps of complex formation have been reviewed in detail in [92] and [100]. The first MSH peptides containing ^{99m}Tc or ^{188}Re were described by Giblin *et al.* [101] who developed an approach with a chelating structure integrated in the sequence of the MSH molecule:

The side-chains of three Cys at positions 3, 4 and 10 in a modified [*D*-Phe^7]-α-MSH$_{3-13}$ sequence together with an amino group can form an NS_3-type chelating structure after appropriate folding of the peptide. As a consequence of the complexation with the radiometal, the initially linear MSH peptide will be cyclized [101]. These cyclic peptides are stable *in vivo* and suitable for targeting melanoma lesions. Alternatively, ^{99m}Tc and ^{188}Re were incorporated into NDP-MSH peptides by complexing $[^{99m}TcO]^{3+}$ with the N_2S_2-type chelator Cys-Gly-Cys-Gly [102, 103] or by complexing with the N_3S-type chelators MAG_2 [103]. The former chelator yielded superior biodistribution results than the latter. Incorporation of ^{99m}Tc and ^{188}Re into MSH peptides was also achieved by complexing $[^{99m}Tc(CO)_3]^+$ with Ala-triazol or $[^{99m}TcO_2]^+$ with tetraamine (N_4) [104]; by complexing $[^{99m}TcO_4]^-$ with HYNIC and tricine or EDDA as coligand [105–107], or by preparation of the $[^{99m}Tc(N)(PNP3)]^{2+}$ building block and formation of a metallated {$[^{99m}Tc(N)]$(Cys-Ahx-β-Ala)} containing cyclic MSH$_{4-13}$ analog [108]. The stability of the latter radiopeptide complex *in vivo* was judged good; however non-specific tissue uptake of ^{99m}Tc was relatively high and thus the potential of the peptide limited.

Linear MSH radiopeptides for melanoma targeting

To date, about 30–40 different linear MSH radiopeptides have been synthesized and examined for melanoma targeting. Table 2 lists the amino acid sequence and biological characteristics of the 15 most prominent linear MSH radiopeptides. DTPA-*bis*MSH (**L1**) was important for the proof of concept [71], including some human studies [73], but it was not stable enough and exhibited high non-specific uptake, not least because of its relatively high molecular weight of ~3500 Da. The general rule to facilitate rapid plasma and kidney clearance and to keep non-target organ accumulation as low as possible is to limit the molecular weight of peptides for targeting at ≤1500 Da. This led to the development of the α-MSH$_{4-10}$ heptapeptide analogs **L2** and **L3** both of which were conjugated to DTPA at the N-terminus [72, 74]. **L3** differed from **L2** by two 2,3-dihydroxy-(2*S*)-propyl (DHP) groups attached to the Lys^{10} side-chain, and it represented the most promising compound of a series of three analogous peptides that either had a free Lys^{10} side-chain (**L2**) or carried one or two DHP groups. The tumor-to-kidney ratio of **L3** in tumor-bearing mice was about 1:2 and the tumor-to-liver ratio about 1:0.4. The same three peptides dimerized via conjugation to DTPA all had inferior targeting properties, particularly very high kidney and liver uptake, as demonstrated for **L4** [74]. Similar observations were made with DTPA-*bis*{NDP-MSH} (**L5**) compared to DTPA-NDP-MSH (**L6**) [109].

Whereas bioactivity and biostability of the MSH fragment analogs of the type of Ac-Nle-Asp-His-*D*-Phe-Arg-Trp-Lys-NH_2 proved to form an excellent basis for further structural modifications, the DTPA chelator showed insufficient binding stability of the radiometal for melanoma targeting. As mentioned, DOTA turned out to be a much more universal cage for different radiometals and, when conjugated to NDP-MSH (**L7**), it only slightly affected the receptor binding affinity of the peptide [110]. The DOTA-octapeptide analog **L8** yielded a more marked drop in affinity and bioactivity which was about 8–10-fold [110]. On the other hand, a comparative study between [^{111}In]DOTA-NDP-MSH (**L7**) and [^{111}In]DOTA-β-Ala-Nle-Asp-His-*D*-Phe-Arg-Trp-Lys-NH_2 (**L8**) showed that **L7** exhibited slower blood clearance together with much higher retention in organs widely distributed in the body, such as muscle, bone, and skin, or sensitive to radiation, such as bone, all of which reduce both the diagnostic and the therapeutic potential of the tridecapeptide [110]. The octapeptide **L8** proved to be stable in experimental animals during the first few hours after injection: Analysis of urine samples at 4 h demonstrated

that all of the radioactivity excreted by renal clearance was bound to intact **L8** whereas at 24 h the excreted radioactivity was bound to smaller fragments [110]. Kidney retention of **L8** was shown to be independent of the presence of MC1R but was associated with the positively charged side-chain of Lys^{10} of the peptide.

The design of [Nle^4,Asp^5,*D*-Phe^7,$Lys(DOTA)^{11}$]-α-MSH_{4-11} (DOTA-NAP-amide) (**L9**) was an important step forward (Fig. **4**), as the MC1R affinity of this radiopeptide was shown to be equivalent to that of α-MSH [79]. *In vivo*, tumor uptake of radiopeptide **L9** was markedly higher than with **L8**, particularly when ^{67}Ga served as radiometal [79]. Conversely, kidney uptake of **L9** was markedly reduced, leading to much improved tumor-to-kidney ratios of 1.1 (for ^{111}In) and 1.8 (for ^{67}Ga). These values were even 65% higher when 15 mg of *L*-Lys were co-injected with the radiopeptide into the animals. It is well known that positively charged peptides interact with the negatively charged surface of proximal tubular cells in the kidneys which enhances re-uptake of the radioligands; competition with basic amino acids reduces re-uptake [111]. Froidevaux *et al.* [79] further demonstrated that high specific radioactivity of the peptide injected (e.g. 185 kBq/20 pg) is decisive for optimal tumor uptake whereas lower specific radioactivity (e.g. 185 kBq/400 pg) reduces tumor uptake considerably but not the non-specific uptake by other tissues [79]. Finally, these studies showed that the major metabolite of **L9** found in urine after renal clearance is Lys([^{111}In]DOTA)-NH_2. Tiny amounts of this metabolite appear already 10–20 min after injection, along with predominating intact **L9**; during the first 24 h, the ratio between **L9** and its metabolite is gradually reversed (Froidevaux, unpublished).

The excellent melanoma specificity of NAP-amide was confirmed by PET imaging studies using [^{68}Ga]DOTA-NAP-amide (**L9**) [79] and [Lys([^{18}F]SFB)^{11}]-NAP-amide (**L10**) [112], although tumor uptake of **L10** was judged moderate [113]. Yet, very tiny tumor lesions in experimental animals are difficult to visualize by PET, and in addition, PET cannot differentiate between melanotic and amelanotic melanoma which is important if an approach with MBPs is considered for treatment. In order to analyze the extent of targeting of melanoma lesions in different organs by **L8** and **L9**, tumors were generated in the skin, the lungs and the liver. In a first study, experimentally induced “primary” intracutaneous melanoma in mice was demonstrated to take up radiolabeled **L8** or **L9** throughout the entire tumor lesion with little radioactivity found in the surrounding healthy tissue (Fig. **5**). In the same way, high specificity was also observed for metastatic melanoma lesions in the lung and the liver, both for melanotic and amelanotic melanoma (Fig. **6**). This demonstrates that the excision and analysis of tumor tissue after application of a diagnostic radiopeptide represents an important complementary method for the proof of the targeting concept with a specific radiopeptide.

Refinement of the structure of NAP-amide is essential to increase the specificity of melanoma targeting by radiolabeled MSH peptides. Options for structural modifications include cyclization (see below), different types of capping of the N- and C-terminal part of the molecule, alterations of the hydrophilicity/hydrophobicity, e.g. by insertion of sugar moieties, or an optimized distribution of positive and negative charges across the molecule. A systematic study on the type of chelator and its conjugation to the MSH peptide is important as well. From our own observation we assume that by introducing a cleavage site in the linker region specific for enzymes of the tubular system of the kidneys, the non-specific accumulation in this organ may be reduced. The positive charge of a free $Lys^{10/11}$ side-chain of MSH analogs exerts an adverse effect on kidney retention *in vivo* (although it enhances receptor binding). This adverse effect is eliminated when the positive charge is neutralized by attaching a small protecting group

such as formyl or acetyl, or by conjugation of the chelator to the ε-position of lysine [114].

The issue of increasing receptor affinity of linear MSH peptides and hence the efficiency of tumor targeting was approached in two ways: Firstly, four dimerized DOTA-MSH hexapeptide analogs (Nle-Asp-His-*D*-Phe-Arg-Trp-NH_2) (**L11**) were prepared by conjugation via a short PEG-linker in either NC-NC orientation (i.e. N-terminus of the first moiety conjugated to the C-terminus of the second) or in CN-NC orientation; the DOTA was attached at the N- or C-terminal end or in the middle of the dimer [115]. While all DOTA-peptides exhibited increased receptor affinity *in vitro*, up to 6-fold for *di*-hexa-(NC-NC)-Gly-Lys(DOTA)-NH_2 in human melanoma cells, tumor uptake *in vivo* was lower than that of DOTA-NAP-amide and non-specific uptake by the kidneys, liver and other organs was high, most likely owing to the increased hydrophobicity and the higher molecular weight of the dimers. In the second approach, six glycosylated derivatives of DOTA-NAP-amide containing galactosyl, glucosyl or maltotriosyl at either the N-terminus, the side-chains of Asp^5 or Lys^{11}, or at the C-terminus were synthesized and tested *in vitro* and *in vivo* [116]. Again, receptor affinities were high for all compounds but the tumor selectivity of five of the six ^{111}In-labeled analogs was inferior to that of DOTA-NAP-amide. By contrast, Gal-DOTA-NAP-amide (**L12**) with the galactosyl at the N-terminus and the DOTA on the Lys^{11} side-chain (Fig. **4**) displayed a 20% improved tumor-to-kidney ratio (Table 2). This demonstrates that the task of “fine-tuning” high-affinity MSH radiopeptides to excellent biological characteristics *in vivo* is complex and requires numerous experiments.

The overall net charge and the charge distribution across the MSH molecule is another important factor that affects the *in vivo* characteristics of linear MSH radiopeptides. Froidevaux *et al.* [114] designed a series of DOTA-NAP-amide analogs by insertion of small alterations, such as the position of DOTA in the peptide and the net charge of the MSH analog, by modifying the C-terminal Lys^{11} residue at both the α- and ε-position. The only peptide with DOTA at the N-terminus showing similar characteristics to those of DOTA-NAP-amide was **L13** (Table 2) with a blocked Lys^{11} side-chain. Introduction of negative charges at the C-terminus did not positively affect the biodistribution data of the corresponding ^{111}In-labeled compounds. These findings were recently confirmed in a study investigating an overall net charge of −1 and −2 for MSH radiopeptides [117]: Whereas DOTA-NAP-*D*-Asp-*D*-Asp (Ac-Nle-Asp-His-*D*-Phe-Arg-Trp-Gly-Lys(DOTA)-*D*-Asp-*D*-Asp-OH) with three negative charges at the C-terminal end and an overall net charge of the molecule of −2 led to a >10-fold drop in MC1R affinity and a markedly lower tumor-to-kidney ratio, compound **L14** with the structure DOTA-Gly-Tyr(P)-Nle-Asp-His-*D*-Phe-Arg-Trp-NH_2 (DOTA-Phospho-MSH_{2-9}; Table 2) and two negative charges in the N-terminal region (overall net charge −1) displayed equivalent biological data to those of DOTA-NAP-amide both *in vitro* and *in vivo*. Yet, the kidney retention was 44% lower; and over an observation period from 4–48 h, the tumor-to-kidney ratio of **L14** was 35% more favorable than that of the reference compound and is currently the highest for short linear MSH radiopeptides [117]. From a comparative analysis of different analogs of DOTA-NAP-amide covering an overall net charge between −2 and +2, it is evident that a net charge greater than −1 or +1 leads to an unfavorably high kidney uptake and reduced tumor uptake with ensuing low tumor-to-kidney ratios (Fig. **7**). For net charges of α-MSH analogues between -1 and +1, the *in vivo* characteristics depend on the charge distribution within the molecule and lipophilicity aspects.

Cyclized MSH radiopeptides for melanoma targeting

The first cyclic α-MSH analog, *cyclo*[Cys^4–Cys^{10}]-α-MSH, was reported by Sawyer *et al.* [118] in 1982 and thought to be 10,000-fold more active than α-MSH. This value was later corrected to equipotency or a value up to 10-fold higher than that of the native peptide, depending on the assay used [47, 119]. Replacement of the *L*-Phe^7 residue in *cyclo*[Cys^4–Cys^{10}]-α-MSH$_{4-12}$ by *D*-Phe^7 led to a potent analog with prolonged activity [119]; it was the basis for the design of even shorter cyclic MSH peptides containing either a cystin (4–10) bridge or a lactam (5–10) bridge with Asp^5 or Glu^5 side-chains coupled to Lys^{10}, Orn^{10}, Dab^{10} or Dpr^{10} [120]. A prominent cyclic MC1R agonist with Asp^5–Lys^{10} ring formation is melanotan II, Ac-Nle^4-*cyclo*[Asp^5,*D*-Phe^7,Lys^{10}]-α-MSH$_{4-10}$, which was shown to exhibit high potency *in vitro* [121] and became the basis for some of the cyclic MSH radiopeptides (see below). Melanotan II itself has not obtained approval for medical use, similar to melanotan I, but it is sold via the internet and used for tanning.

In the following sections, cyclic MSH radiopeptides obtained through rhenium-induced ring formation, lactam-bridge or “click” cyclization will be presented, followed by RGD-hybride cyclic MSH radiopeptides and MSH radiopeptides developed for therapy.

Rhenium-cyclized MSH radiopeptides

As already outlined, Giblin *et al.* [101] designed and tested Cys-containing α-MSH analogs with which ^{99m}Tc and ^{188}Re radiometals can be stably complexed through coordination with structures that form an integral part of the peptide itself. These authors set out with a comparison of the conformation and biological characteristics of *cyclo*[Cys^4–Cys^{10},*D*-Phe^7]-α-MSH$_{4-13}$, ReO-{[Cys^{4,10},*D*-Phe^7]-α-MSH$_{4-13}$} (ReMSH) and ReO-{[Cys^{3,4,10},*D*-Phe^7]-α-MSH$_{3-13}$} (ReCCMSH) (**C1**; Table 3). The latter displayed an IC$_{50}$ of 2.9 nM in the mouse B16-F1 melanoma cell binding assay and stable complex formation with ^{99m}Tc and ^{188}Re. (It is interesting to note that ReO-cyclization of the peptide increased receptor affinity whereas in subsequent publications also a decrease of IC$_{50}$ after cyclization was found, depending on the cell type used.) In a murine melanoma model, [^{99m}Tc]CCMSH showed significant tumor uptake and was effective in imaging the tumor although uptake by the kidneys and other organs was relatively high [101]. Replacement of the Lys^{11} residue in ReCCMSH by Nle^{11} or Gly^{11} dramatically decreased kidney uptake but markedly reduced tumor uptake [122]. The authors concluded that co-infusion of *L*-Lys is a better approach to reduce kidney uptake than to replace the Lys^{11} side-chain in ReCCMSH; they also found that linear [^{99m}Tc]CGCG-NDP-MSH exhibited lower tumor and lower kidney uptake but higher uptake by the intestines than [^{99m}Tc]ReCCMS because of excretion via the gastrointestinal tract of [^{99m}Tc]CGCG [122].

Replacement of Lys^{11} of **C1** by Arg^{11} yielded [^{188}Re][Arg^{11}]ReCCMSH (**C2**) that displayed high receptor affinity (IC$_{50}$ 1.9 nM), very good tumor uptake and markedly lower kidney uptake [123]. Co-infusion of 20 mg *L*-Lys per animal further reduced kidney uptake, increasing tumor-to-kidney ratio to 2.5 at 1 h post-injection [123]. Biodistribution experiments with ^{188}Re-labeled **C1** and **C2** in Scid mice bearing a human melanoma TXM13 xenograft gave similar results as found previously for B16-F1 melanoma: Both **C1** and **C2** showed similar tumor uptake and retention but kidney uptake was twice as high for **C1** compared to **C2** [124]. Peptide **C2**, N-terminally extended by Ac-Lys- or Ac-*D*-Lys, also served as template for radioiodination by attachment of [^{125}I]-iodobenzoate

([^{125}I]-IBA) at the ε-position of the lysines [125]. In particular the peptide with Ac-*D*-Lys displayed excellent *in vitro* uptake and retention by B16-F1 melanoma cells as well as by experimental tumors *in vivo*. By contrast, NDP-MSH labeled with [^{125}I]-IBA was released from the cells and also from the tumor very quickly and hence is not suitable for tumor localization studies [122, 125]. The data clearly demonstrate that rhenium cyclization significantly enhances MSH trapping in the cell and thus facilitates tumor localization with iodine radionuclides.

(Ala-triazol)Ac-Re[Arg^{11}]CCMSH (**C3a**; Fig. **8**) and N_4-CO-Re[Arg^{11}]CCMSH (**C3b**; Table 3) were designed to combine a chelator for ^{99m}Tc with ReO-cyclized **2** [104]. Radiolabeling of these peptides proceeded via [^{99m}Tc(CO)$_3$]$^+$ for **C3a** and [^{99m}TcO)$_2$]$^+$ for **C3b**, respectively. Both compounds showed high radiochemical stability and MC1R affinity. Tumor targeting *in vivo* was selective with good retention in the tumor, particularly for **C3a**, making it possible to clearly visualize melanoma tumors by PET (Fig. **9**).

ReO-{[Cys^{3,4,10},*D*-Phe^7]-α-MSH$_{3-13}$} (ReCCMSH; **C1**) containing non-radioactive (Re=O)$^{3+}$ served as lead compound for the development of stable cyclic DOTA-containing MSH radiotracers. The first of a series of analogs was [^{111}In]DOTA-ReCCMSH (**C4**; Table 3) that showed considerably higher tumor uptake and markedly lower kidney uptake than the corresponding linear peptides which make **C4** a potential candidate for radiodetection and radiotherapy [126]. **C4** exhibited very good MC1R affinity (IC_{50} of 1.2 nM). Comparison of ^{99m}Tc-labeled **C1** with ^{111}In-labeled **C4** demonstrated that uptake and elimination of **C1** from the tumor and non-specific tissues is faster than those of **C4** which has a longer residence time in the tumor but also in the kidneys [127]. In order to lower kidney uptake further, Cheng *et al.* [128] undertook a structure-activity study and designed four new analogs (Ac-Lys(DOTA)-ReCCMSH, DOTA-Re[Arg^{11}]CCMSH, DOTA-ReCCMSH-OH, DOTA-ReCCMSH-Asp-OH) in order to compare the introduction of a delocalized positive charge in position 11 with additional negative charges (−1, −2) at the C-terminus. Undoubtedly, DOTA-Re[Arg^{11}]CCMSH (**C5**) turned out to be the most promising because it showed high tumor uptake combined with considerably reduced kidney uptake; tumor-to-kidney ratios were 1.8 after 0.5 h, 2.0 after 2 h, 2.4 after 4 h and still 1.5 after 24 h [128]. Instead of labeling **C5** with ^{111}In, McQuade *et al*. [129] used ^{86}Y and ^{64}Cu for a comparative study which showed that both radiopeptides exhibited similar characteristics in melanoma targeting as ^{111}In-labeled **C5**, except that the ^{64}Cu-labeled compound yielded more non-specific tissue uptake. As DOTA is not an ideal chelator for ^{64}Cu, CBTE2A was attached to Re[Arg^{11}]CCMSH to produce [^{64}Cu]CBTE2A-Re[Arg^{11}]CCMSH (**C6**; Table 3) [97]. Biodistribution data of this radiotracer were much improved as only little non-specific uptake was observed, except for the kidneys. Tumor lesions could be visualized well by PET imaging and microimaging. Similarly, ^{68}Ga was complexed to peptide **C5** which turned out to be a promising PET agent for early detection of melanoma [130].

A comparison between **C2** and **C5** by Miao *et al.* [131] revealed that both radiopeptides, [^{99m}Tc][Arg^{11}]CCMSH and [^{111}In]DOTA-Re[Arg^{11}]CCMSH, are promising candidates for the detection of melanoma metastases, whereby the former produced better resolution of lesion images than the latter. Another candidate for melanoma detection is [^{203}Pb]DOTA-Re[Arg^{11}]CCMSH that was developed as imaging surrogate for [^{212}Pb]DOTA-Re[Arg^{11}]CCMSH envisaged for melanoma treatment [132] (see below). The synthesis of [Arg^{11}]CCMSH analogs with the N-terminus extended by Gly-Gly-Nle or truncated at the C-terminus showed that Arg^{11}-Pro^{12} residues were required for efficient

tumor targeting whereas N-terminal extension positively affected the reduction of kidney uptake [133].

Lactam-bridge and "click" cyclized MSH radiopeptides

The first lactam-bridge cyclized MSH radiopeptides for imaging were prepared in 2008, when Raposinho *et al.* [134] coupled the ^{99m}Tc-chelator pyrazolyl diamine Pz^1 to β-Ala-extended melanotan II and labeled the conjugate with [^{99m}Tc(CO)$_3$]$^+$, yielding [^{99m}Tc(CO)$_3$]-Pz^1-β-Ala-Nle-*cyclo*[Asp-His-*D*-Phe-Arg-Trp-Lys-NH$_2$]. This radiopeptide showed good tumor uptake, but very high kidney values in the first few hours after injection. Although the larger portion of accumulated radionuclide in the kidneys was eliminated by 24 h post-injection, the characteristics of this radiopeptide were not yet comparable to those of the best Re-cyclized MSH analogs. Concurrently with these studies, Miao *et al.* [135] synthesized DOTA-*cyclo*[Lys-Nle-Glu-His-*D*-Phe-Arg-Trp-Gly-Arg-Pro-Val-Asp] (DOTA-*cyc*MSH) and DOTA-Gly-Glu-*cyclo*[Lys-Nle-Glu-His-*D*-Phe-Arg-Trp-Gly-Arg-Pro-Val-Asp] (DOTA-Gly-Glu-*cyc*MSH) both of which were labeled with ^{111}In. These peptides displayed fairly good tumor uptake as well, but again with the impairment of high kidney values. Extension of the cyclic dodecapeptide ring structure of DOTA-*cyc*MSH by the dipeptide Gly-Glu to form DOTA-Gly-Glu-*cyc*MSH reduced kidney uptake by 40–50%. This kind of structural element was successfully used later for cyclic MSH analogs with smaller ring size. Labeling of the cyclic 12-residue DOTA-Gly-Glu-*cyc*MSH with ^{111}In and ^{67}Ga produced two radiopeptides apparently useful for imaging of primary and metastatic melanoma in tumor-bearing mice [136, 137] but with insufficient tumor-to-kidney ratios. By shifting the DOTA chelator from the N-terminus to the C-terminus of DOTA-Gly-Glu-*cyc*MSH, a radiopeptide with even better tumor selectivity was obtained [138], but again kidney values were still very high which prompted Guo *et al.* [139] to focus on cyclic MSH peptides with smaller ring size.

The melanotan-II-type lactam-bridged ring structure served as template for three new analogs: DOTA-Nle-*cyclo*[Asp-His-*D*-Phe-Arg-Trp-Lys-NH$_2$] (**C7**; Table 3) [139], DOTA-Gly-Gly-Nle-*cyclo*[Asp-His-*D*-Phe-Arg-Trp-Lys-NH$_2$] (**C8**) [140], NOTA-Gly-Gly-Nle-*cyclo*[Asp-His-*D*-Phe-Arg-Trp-Lys-NH$_2$] (**C9**) [141] which exhibited increasingly superior characteristics from **C7** to **C9** when studied *in vivo* for melanoma targeting. In particular **C8** and **C9** became new lead compounds with comparable or even somewhat superior characteristics to those of Re-cyclized MSH analogs. A comparison of the N-terminal dipeptide extension of melanotan II by either Gly-Gly or Gly-Glu showed that the latter had a 10-fold lower receptor affinity than the former, which resulted in inferior biodistribution data [140]. Therefore, Gly-Gly served as optimal N-terminal extension. Replacement of the DOTA chelator by NOTA slightly increased MC1R affinity and further improved tumor-to-kidney ratios for a ^{67}Ga-labeled **C9** that produced values up to >2.5 [141]. Analogous observations were made with ^{64}Cu-labeled **C9** produced for PET imaging [142]: Tumor-to-kidney ratios gradually increased from 1.35 to 5.74 between 0.5 h and 24 h post-injection and surpassed the values obtained with **C6** and **C8** 2- to 5-fold. In fact, they ranged amongst the highest values obtained for MSH radiopeptides to date. Not surprisingly labeling of **C8** with ^{177}Lu (which requires DOTA as chelator) yielded lower tumor-to-kidney values [143]; nevertheless, the biodistribution characteristics of this compound were judged potentially promising for ^{177}Lu-therapy [143].

Instead of using lactam bridge formation between residues 5 and 10, cyclization of α-MSH$_{4-10}$ peptides can be achieved by copper-catalyzed terminal azide-alkyne cycloaddition "click" chemistry techniques: Martin *et al.* [144] designed click-melanotan II

(ClickMTII), Ac-Nle-*cyclo*[Pra-His-*D*-Phe-Trp-Lys(N_3)-NH_2], and four DOTA-containing ClickMTII analogs by triazol formation between the Pra^5 and $Lys(N_3)^{10}$ residues, followed by attachment of DOTA either to the N-terminal amino group or the ε-side-chain amino group of an additional Lys attached to Lys^{10} or, alternatively, to the Gly-Gly spacer-extended N- or C-terminal attachment points. Except for DOTA-ClickMTII, all DOTA other analogs of ClickMTII exhibited high MC1R affinity, excellent stability and good tumor uptake. The highest tumor-to-kidney ratio was obtained with [^{68}Gal]DOTA-Gly-Gly-Nle-*cyclo*[Pra-His-*D*-Phe-Trp-Lys(N_3)-NH_2] (**C10**; Table 3) which produced clear PET images [144].

Improvement of the original ^{99m}Tc-labeled melanotan II, [^{99m}Tc(CO)$_3$]-Pz^1-β-Ala-Nle-*cyclo*[Asp-His-*D*-Phe-Arg-Trp-Lys-NH_2] (see above), by a structure-activity study to find a superior chelator for ^{99m}Tc resulted in a compound containing the following pyrazolyl group: 4-{*N*-[2-(4-(2-carboxyethyl)-3,5-dimethyl-1*H*-pyrazol-1-yl)-ethyl], *N*-[(2-amino)ethyl]}amino-butanoic acid (Pz^4) [145]. This MSH radiopeptide, [^{99m}Tc(CO)$_3$]-Pz^4-β-Ala-Nle-*cyclo*[Asp-His-*D*-Phe-Arg-Trp-Lys-NH_2] (**C11**; Table 3), yielded lower kidney and liver uptake and presented the highest tumor-to-kidney ratio ever found (7.1 at 4 h post-injection). Consequently, excellent scintigraphy images were obtained [145]. Attachment of other types of ^{99m}Tc chelators to Gly-Gly-Nle-*cyclo*[Asp-His-*D*-Phe-Arg-Trp-Lys-NH_2] such as [^{99m}Tc]MAG_3, [^{99m}Tc]$AcCG_3$, [^{99m}Tc(CO)$_3$]HYNIC or [^{99m}Tc](EDDA)-HYNIC showed that the latter exhibited the highest melanoma uptake and fastest urinary clearance, combined with good tumor localization [146]; yet, the *in vivo* characteristics did not match those of **C11**. If however the N-terminal Gly-Gly extension of melanotan II was replaced by 8-amino-octanoic acid (Aoc), the resulting [^{99m}Tc](EDDA)-HYNIC-Aoc-Nle-*cyclo*[Asp-His-*D*-Phe-Arg-Trp-Lys-NH_2] (**C12**; Table 3) showed high MC1R affinity, high melanoma uptake und markedly reduced kidney uptake, matching the tumor-to-kidney ratios of **C11** [147]. Other spacers in the place of Aoc did not reproduce the data obtained with **C12**. Analogous imaging results were also obtained with M21 human melanoma xenografted into nude mice [148].

Gao *et al.* [99] used a different approach for a lactam-cyclized ^{64}Cu-labeled NOTA-MSH radiopeptide: [Lys^4,*D*-Phe^7,Glu^{10},Arg^{11}]-α-MSH_{4-13} was cyclized between residues 4 and 10, yielding an analog in which the negative charge in position 5 and the positive charge in position 11 of the α-MSH molecule were maintained. NOTA was attached to the N-terminus extended by the linker Ahx-β-Ala, using NOTA-Bz-NCS as reagent. This cyclic MSH analog exhibited an approx. 20- to 40-fold lower K_i (whether or not NOTA or [Cu]NOTA was present) than linear Ahx-β-Ala-[Nle^4,*D*-Phe^7]-α-MSH_{4-10} with and without NOTA attached [103]. It should be noted, however, that the cyclic peptide had a different C-terminus and a higher molecular weight than the linear peptide. A more informative comparison was reported by Carta *et al.* [108] who synthesized linear H-Cys-Ahx-β-Ala-[Lys^4,*D*-Phe^7,Glu^{10},Arg^{11}]-α-MSH_{4-13} and the corresponding (4–10) lactam-cyclized Cys-Ahx-β-Ala-*cyclo*[Lys^4,*D*-Phe^7,Glu^{10},Arg^{11}]-α-MSH_{4-13}. Radiolabeling was done as outlined above by formation of a stable radiometal complex {[^{99m}Tc(N)](Cys-Ahx-β-Ala)}-peptide using PNP3. *In vitro* and *in vivo* analysis demonstrated that the linear peptide displayed a >100-fold higher MC1R affinity and much more favorable biodistribution characeristics than the cyclic compound. Hence, whether the cyclic or linear form of a peptide is to be preferred depends on structural details that cannot be generalized but have to be examined experimentally.

RGD-hybrid cyclized MSH radiopeptides

The finding by Capello *et al.* [149] that the RGD motif Arg-Gly-Asp, integrated into a somatostatin analog used for scintigraphy, can increase the radiotherapeutic efficacy of the radiopeptide by dual targeting, thus leading to a higher tumoricidal effect, prompted Yang *et al.* [150] to synthesize RGD-Lys-[Arg^{11}]CCMSH and label it with ^{99m}Tc to yield cyclic [^{99m}Tc]-RGD-Lys-[Arg^{11}]CCMSH. The peptide exhibited good tumor uptake *in vivo* and prolonged tumor retention but also high kidney uptake which could be reduced by co-injection of *L*-Lys. Single treatment of cultured B16-F1 melanoma cells with the radiotracer for 3 h showed significantly reduced survival (65%) of the cells [150]. Application of this radiotracer to M21 human melanoma xenografted into nude mice led to tumor uptake that could be partially blocked by coinjection of either RGD or [Arg^{11}]CCMSH; kidney uptake was very high [151]. Modification of the RGD motif in the RGD-Lys-[Arg^{11}]CCMSH molecule by exchange of Gly for Ala had a positive effect on tumor uptake; kidney uptake remained high but tumor lesions could be visualized clearly [152]. Similarly, high kidney uptake was also observed when Gly was exchanged for Thr or Val in the RGD motif [153]. When the Lys residue linking the RGD motif to [Arg^{11}]CCMSH was replaced by an Arg residue, tumor uptake was increased and kidney uptake reduced, whereby the latter was still 2-fold higher than the former [154]. A similar reduction of kidney uptake was found for the peptide analog with an Arg linker and the RAD motif [155]. Elimination of the Lys linker or replacement by Gly reduced kidney uptake considerably and yielded tumor-to-kidney ratios ranging between ~0.6 at 2 h and ~2 at 24 h post-injection [156]. β-Ala, Ahx, Aoc or PEG were suitable linkers replacing Lys for conjugation of a series of RXD, XAD and cyclic RGD motifs to [Arg^{11}]CCMSH (**C13**; Table 3). These peptides generally led to improved tumor targeting [157–159]. In summary, the dual targeting approach by RGD-MSH radiopeptides simultaneously interacting with integrin receptors and with MC1R has led to the development of some promising MSH analogs, but the ideal structure of the conjugate surpassing previous MSH radiotracers warrants further development.

Therapy studies with MSH radiopeptides

Melanoma targeting for therapy requires peptides that contain α-emitting (e.g. ^{212}Pb) or high-energy β-emitting radionuclides (e.g. ^{90}Y, ^{177}Lu, ^{67}Cu, ^{188}Re) or isotopes that emit Auger electrons (e.g. ^{99m}Tc, ^{111}In) [92, 160-162]. Whereas the literature on basic studies with ^{99m}Tc- and ^{111}In-labeled MSH peptides is abundant, reports on potential therapeutic applications of MSH peptides labeled with ^{90}Y, ^{177}Lu, ^{67}Cu, ^{188}Re, or ^{212}Pb is scarce. A first important issue was a comparative analysis of ^{90}Y- and ^{177}Lu-labeled MSH peptides *in vitro* and *in vivo*. Cellular internalization and retention of [^{90}Y]DOTA-Re[Arg^{11}]CCMSH and [^{177}Lu]DOTA-Re[Arg^{11}]CCMSH in B16-F1 melanoma cells was fast and retention of the radioactivity extended [163]. In B16-F1 melanoma-bearing C57 mice high receptor-mediated tumor uptake and retention coupled with fast whole-body clearance was noted; little activity accumulated in normal organs except for the kidneys [163]. These data indicated that both radiopeptides may prove suitable for targeted radionuclide therapy of melanoma, in particular after coupling of a negatively charged amino acid residue (Glu) at their N-terminus with which renal uptake was markedly reduced [164].

Treatment of mouse B16-F1 melanoma-bearing C57 mice with 2x 18.5 MBq (4 days apart) or 1x 37 MBq of [^{177}Lu]DOTA-Re[Arg^{11}]CCMSH led to tumor volumes that were 26% and, respectively, 30%, smaller than those in control animals. The mean survival times of the animals increased by 15% and 21%, respectively [165]. Similar studies

using doses of 7.4, 22.2, or 2x 14.8 MBq (3 days apart) of [^{188}Re][Arg^{11}]CCMSH showed tumor volumes that were 17%, 27.5% or 40% smaller than those of control animals [166]. Mean survival was only extended with the largest dose applied, from 9.4 days to 13.3 days. Interestingly, nude mice bearing TXM13 human melanoma treated with 22.2, 2x 14.8 (7 days apart), or 37.0 MBq of [^{188}Re][Arg^{11}]CCMSH experienced marked extension of survival, from 39.6 days to 72.7 days for the largest single dose, to 57.6 days for 22.2 MBq and to only 41.4 days for 2x 14.8 MBq [166]. In the same order, tumor volumes 8 days after treatment were 6.5%, 21.5%, and 47.0%. This demonstrates a greater therapeutic efficacy of [^{188}Re][Arg^{11}]CCMSH in the human melanoma model compared to mouse melanoma.

The α-emitter ^{212}Pb was studied with B16-F1 melanoma-bearing C57 mice by injection of 1.85, 3.7, or 7.4 MBq of [^{212}Pb]DOTA-Re[Arg^{11}]CCMSH [167]. Pharmacokinetic analysis demonstrated that excretion of the radiotracer through the kidneys was rapid and that the dose of ^{212}Pb per gram of tissue was 3-fold higher in the melanoma tumor than in the kidneys 4 h post-injection; the radioactivity in other tissues was negligible. This proved rapid and specific uptake as well as long retention of the radiotracer by the tumor. Survival times of the animals increased from an average of 14.4 days for the controls to 22.0 days (1.85 MBq), 28.0 days (3.7 MBq) and 49.8 days (7.4 MBq). Two of 10 animals (3.7 MBq) and 4 of 9 animals (7.4 MBq) were free of tumor and survived the 120-day study period [167]. These experiments with [^{212}Pb]DOTA-Re[Arg^{11}]CCMSH lead to the expectation that a radiopharmaceutical adapted for human application of targeted radionuclide therapy of melanoma will find its way into the clinic. An important intermediate step will however be to study the efficiency of such a radiopeptide in experimental animals bearing patient-derived orthotopic melanoma xenografts (PDOX). To date, the literature on melanoma PDOX studies in general is very scarce and missing entirely for radiotherapy studies.

Perspectives and limitations of melanoma targeting with MSH radiopeptides

As already outlined, renal accumulation is *the* predominant problem for all radiopeptides containing metal chelators such as DOTA or DTPA and is not confined to MSH analogs. The most frequently used radiopeptide in the clinic, both for diagnostic and therapeutic application, is ^{111}In-, ^{68}Ga-, ^{90}Y- or ^{177}Lu-labeled DOTA-octreotide (DOTATOC) [168]. Yet, severe renal complications (such as delayed renal insufficiency) have been reported even after a moderate cumulative dose of ~5,600 MBq/m^2 of [^{90}Y]DOTATOC used for treatment of neuroendocrine tumors [169]. For these reasons, a number of improved somatostatin radiopeptides have been developed in the past few years [170], but research still continues to find more suitable compounds with the lowest possible kidney uptake and retention.

An analogous situation is found for MSH radiopeptides developed for melanoma targeting: Kidney uptake and retention of considerable amounts of the injected dose of many of the compounds presented in this review will limit the therapeutic efficacy of this approach. In most of the published studies with DOTA-MSH radiopeptides, the uptake of radioactivity by the kidneys usually exceeds that of the tumor. However in the past ten years, novel MSH radiopeptides have become available that exhibit higher uptake by the tumor than by the kidneys. Yet, as volumes of melanoma tumor lesions in the clinical situation of patients are generally smaller than those of the kidneys, the problem of accumulated radiotoxicity still persists, even though various methods to reduce renal retention have been developed. A question which is not yet solved at present relates to

the molecular processes of retention of radiopeptides by the kidneys. If eventually reabsorption of radioactive MSH by proximal tubules can be inhibited specifically, therapeutic application of MSH radiopeptides may be envisaged. Another approach that may circumvent kidney retention of radiopeptides but has barely been investigated for melanoma targeting, is pretargeting of the tumor lesions with a non-radioactive MSH peptide conjugate whose cell uptake is slow and that carries a marker group, e.g. biotin, which in a second step can be targeted with the radionuclide bound to the counterpart of the marker group, e.g. avidin. A study using a pretargeted bivalent bacteriophage revealed that this principle can work for melanoma [171], although considerable non-specific accumulation in the intestinal tract was noted for this particular case. Further development of the pretargeting approach may be worthwhile.

For diagnostic application of MSH radiopeptides, the situation is different because the load of radioactivity, in particular for a single analysis by PET, is much smaller. Tables 2 and 3 show a collection of interesting MSH candidates for melanoma diagnosis which may eventually be developed for clinical application. Additional information is also found in [172]. MSH radiopharmaceuticals may complement magnetic resonance imaging or computed tomography methods for addressing specific diagnostic questions, e.g. when more information about tumor lesions is needed. Thus, there is certainly a considerable interest for introducing receptor-based melanoma imaging in the clinic.

Another important aspect that may limit the melanoma targeting approach with MSH radiopeptides is the expression of MC1R in non-melanoma cell types and tissues as well as the crossreaction of MSH radiopeptides with other MC receptor subtypes such as MC3R, MC4R, and MC5R. For example, MC1R is not only expressed on melanocytes and melanoma cells but also on macrophages, neutrophils, endothelial cells, astrocytes, and adipocytes [173-175], although generally to a lesser degree than on melanocytes. Yet, studies in experimental animals have demonstrated that accumulation of MSH radiopeptides in skin tissue (containing melanocytes) surrounding melanoma tumors is very low [79, 110] and well tolerated during and after therapy [167]. Thus, as melanoma radiotherapy will always be an *ultima ratio* approach when no other options can help, a low degree of non-specific accumulation of radioactivity is tolerable. With respect to the protection of leukocytes (macrophages, neutrophils) where MSH peptides exert an anti-inflammatory function, careful selection of MSH radiopeptides with a decreased affinity to MC3R (the predominant MC receptor on macrophages [172]) will further reduce or avoid damage.

DIRECT TARGETING OF MELANIN WITH PEPTIDES, SMALL MOLECULES OR ANTIBODIES

Direct targeting of melanin was based on the efforts to develop melanoma-specific radioimmunotherapy (RIT) approaches for treating experimental and clinical melanoma. The first studies of RIT date back to the early 1980s when monoclonal antibodies (mAbs) against a high-molecular weight antigen (a melanoma tumor-associated proteoglycan) were developed and labeled with ^{131}I with which melanoma lesions could be treated in experimental animals and some patients [176, 177]. In the past two decades, mAbs labeled with α-and β-emitting radionuclides and targeted to different melanoma antigens were investigated clinically; detailed historical accounts are found in references [86] and [178]. The generation of the murine mAb 6D2 that binds to melanin of the fungus *Cryptococcus neoformans* [179] initiated a study by Dadachova *et al.* [180]

who demonstrated that ^{188}Re-labeled 6D2 specifically targets extracellular melanin in MNT1 human melanoma transplanted to nude mice. Tumor growth was inhibited by labeled 6D2 and survival of treated animals prolonged. Also, there was no crossreaction of 6D2 with normal melanized tissues in black mice [180]. Preclinical and clinical studies with [^{188}Re]-6D2 demonstrated that the antibody is effective over a wide range of melanin concentrations in tumors [86] and that it is taken up by tumors in patients and the various sites of metastatic lesions, without any accumulation in healthy melanized tissues such as eye, skin or melanized neurons; and finally, it led to prolongation of the patients' survival [181].

Melanin-binding radiopeptides for melanoma targeting

The positive results obtained with the [^{188}Re]-6D2 mAb for a small patient group encouraged Dadachova *et al.* [182] to investigate the melanin-binding peptide (MBP) 4B4 (Tyr-Gly-Arg-Lys-Phe-Trp-His-Gly-Arg-His; [85]) for MBPT-type melanoma targeting. HYNIC-4B4 was synthesized using *D*-amino acids for all residues (all-*D*-4B4) in order to increase serum stability; similarly, a control decapeptide was prepared from *D*-amino acids. The compounds were labeled with ^{188}Re and applied to nude mice bearing MNT1 human melanoma tumors. The results showed that [^{188}Re]HYNIC-4B4 only bound to non-viable melanoma cells, i.e. they did not cross the cell membrane [182]. Administration of 2x 37 MBq of [^{188}Re]HYNIC-4B4 in a 10- to 20-day interval significantly retarded tumor growth. Although uptake by the kidneys and other organs was high, no histological damage was observed, and there was no accumulation of radiotracer in melanized healthy tissues of black mice [182]. In order to reduce kidney uptake, MBPs with shorter chain-lengths were identified using a phage-display library [183]. Three heptapeptides bound to melanin and served as leads for the preparation of the corresponding HYNIC-conjugated all-*D*-heptapeptides that were labeled with ^{188}Re. Binding analysis with MNT1 and A2058 human melanoma cells and *in vivo* biodistribution studies with nude mice bearing A2058 melanoma revealed that the [^{188}Re]HYNIC-Asn-Pro-Asn-Trp-Gly-Pro-Arg heptapeptide showed the most promising data for treatment. In a therapy study, nude mice bearing A2059 tumors were treated with 37 MBq of [^{188}Re]HYNIC-Asn-Pro-Asn-Trp-Gly-Pro-Arg and, for comparison, with [^{188}Re]HYNIC-4B4 after the tumors had reached a size of 0.7-0.8 cm in diameter. Treatment with the radioligands was repeated 7 days later. An identical significant retardation of tumor growth was observed for both radiotracers; kidney uptake was however 7-fold lower with the heptapeptide compared to 4B4 [183]. Thus, MBP-heptapeptides may serve as vehicles for transport of radionuclides into melanoma tumor lesions.

Melanin-binding with small radiolabeled molecules for melanoma targeting

The lack of penetration of the MBP-decapeptide and the heptapeptides into melanoma cells increased the interest in small molecules such as radiolabeled benzamides that bind to melanoma tumors with good retention and localization properties by intracellular integration into melanin (reviewed in [86]). One of these benzamides is MIP-1145, *N*-(2-diethylamino-ethyl)-4-(4-fluoro-benzamide)-5-iodo-2-methoxy-benzamide, which after labeling with ^{131}I and injection into melanoma-bearing animals dramatically inhibited tumor growth [184]. A clinical study with ^{123}I- and ^{131}I-labeled BA52, benzo-(1,3)-dioxolo-5-carboxylic acid (4-(2-diethylamino-ethylcarbamoyl)-2-iodo-5-methoxy-phenyl)-amide, demonstrated the potential of melanin-binding benzamides for imaging and

therapy of patients with metastatic melanoma [185]. Thus, small molecules, peptides and mAbs binding to melanin may all be conceived – as single drugs or in combination with others – for specific application in the treatment of metastatic melanoma.

PEPTIDE-PHOTOSENSITIZER CONJUGATES FOR PHOTODYNAMIC THERAPY OF MELANOTIC LESIONS

Principles of photodynamic therapy with peptide-photosensitizer conjugates

In last few decades, photodynamic therapy (PDT) has received considerable attention, especially in the field of skin cancer treatment, e.g. for actinic keratosis and superficial BCC, SCC, macular degeneration etc. [186]. PDT is favored over other therapeutic modalities owing to its non-invasive nature and because light of different wavelengths represents a decisive component of treatment. The different wavelengths of light differ in their ability to penetrate the skin; for example, UV light just penetrates the corneal layer and upper part of the epidermis whereas infrared light can reach much deeper layers down to subcutaneous tissue [187,188]. Hence, tunable light is preferred to treat the various skin disorders occurring in different layers, i.e. at different depths of the skin. The other component of PDT are photosensitizers which usually consist of highly conjugated systems that have the capacity to produce reactive oxygen species (ROS) when exposed to certain wavelengths of light. ROS are toxic and can react with neighboring cells and tissues, eventually leading to cell death. A range of photosensitizers approved by the FDA and EU has been reported, e.g. verteporfin, temoporfin [189, 190], HPPH, photofrin and others [186]. There are also FDA-approved precursors of photosensitizers, e.g. δ-aminolevulinic acid (ALA; Levulan) and methyl aminolevulinate (Metvix): After a few hours of topical application of these precursor-drugs, they are integrated in the inherent biosynthetic pathway of cellular synthesis of protoporphyrin IX (PPIX), a photosensitizer [191]. In this way, dormant and hyperactive cancer cells and malignant lesions may be localized, as these cells have an upregulated biosynthesis of PPIX. Light of specific wavelengths can induce cytotoxicity which makes PDT a very attractive tool for treatment of tumor tissues.

PDT can circumvent the unwanted side-effects of radiolabeled peptide ligands in PRRT which are a concern for therapy. For example, early stage skin cancer or tumors in delicate places such as the face, neck, and forehead are preferably treated with a “softer” approach, represented by PDT. To establish targeted PDT, ideally the same peptides are used that have been shown with radionuclides to target specific types of skin cancer. To this end, the chelators for radionuclides in these peptides are replaced by a photosensitizer so that the biological characteristics of the peptide conjugates are more or less maintained, e.g. good binding affinity to MC1R in melanoma. As described above for radiopeptides, newly synthesized photosensitizer-peptide conjugates are vigorously tested for binding and bioactivity, lack of cytotoxicity in the dark and toxicity after exposure to a specific wavelength. Important is the binding of the MSH-photosensitizer conjugates to MC1R and its rapid internalization in melanotic melanocytes and malignant melanoma overexpressing MC1R so that the photosensitizer will get as close to the nucleus as possible. After exposure of the treated skin lesions with light of the appropriate wavelength, the activated photosensitizer will induce the formation of ROS that cause cell death and tissue necrosis (Fig. **10**).

MSH-photosensitizer conjugates

In order to direct the photosensitizer more specifically to the nucleus of cancer cells, Slastnikova *et al.* [192] developed a four-component nanotransporter for melanoma targeting, consisting of bacteriochlorin-p as photosensitizer, an MSH peptide for interaction with MC1R and internalization by the cells, an endosome release unit based on the diphtheria toxin translocation domain and finally the SV40 large T antigen domain for optimized nuclear localization. This relatively large construct, however, was far from being as specific as MSH radiopeptides when studied by *in vivo* biodistribution. Nevertheless, B16-F1 and Cloudman-S91 melanoma-bearing mice responded positively to PDT with this construct; their life-span was markedly increased compared to controls [192].

We chose a different approach by confining the conjugates to just two components, the photosensitizer (e.g. HPPH) and the MSH peptide (NAP-amide). Basically, the DOTA chelator in DOTA-NAP-amide was replaced by HPPH, yielding HPPH-NAP-amide which specifically binds to MC1R (Fig. **11a**). The peptide conjugate was tested for specificity and cytotoxicity using B16-F10 mouse melanoma cells. First, incubation of HPPH-NAP-amide with these cells without exposure to light resulted in a melanin production comparable to that elicited by α-MSH or NAP-amide (Fig. **11b**); HPPH itself did not induce melanogenesis. This indicates that HPPH-NAP-amide is a full agonist of MC1R. In the dark, i.e. in the absence of any light-induced generation of ROS, no cell toxicity was observed using various concentrations of HPPH-NAP-amide (Fig. **11c**; the two concentrations 1 µM and 10 µM are shown, compared to controls). By contrast, exposure of the cells to light promoted cell death (Rout and Bigliardi, unpublished results). These promising preliminary results obtained with a photosensitizer conjugated to a specific ligand for MC1R open up a new area for targeted PDT utilizing laser or incoherent light with specific activating wavelengths tailored to the corresponding photosensitizer. Moreover, exploring suitable peptide-photosensitizer conjugates for various skin disorders including malignant melanoma, hypermelanotic lesions or other types of skin cancer will bring targeted PDT more to the focus of dermato-oncology.

CONCLUSIONS AND PERSPECTIVES

Peptide drugs for skin cancer are of increasing interest, in particular with respect to targeting melanoma and hypermelanotic lesions. In the past 20 years, considerable progress in the design of specific and stable α-MSH radiopeptides has been documented in the literature. The novel MSH compounds display comparable targeting characteristics in experimental melanoma models as achieved with the clinically used somatostatin radiopharmaceuticals. For linear MSH radiopeptides, a first breakthrough was DOTA-NAP-amide which yielded high tumor uptake and a good tumor-to-kidney ratios when studied *in vivo* with melanoma-bearing animals. DOTA-Gal-NAP-amide and DOTA-Phospho-MSH_{2-9} further improved the targeting specificity. With respect to cyclic MSH radiopeptides, the rhenium-cyclized Re[Arg^{11}]CCMSH or DOTA-Re[Arg^{11}]CCMSH, and the lactam bridge-cyclized MSH analogs of melanotan II with the N-terminal extension of DOTA-Gly-Gly, NOTA-Gly-Gly, Pz^4-β-Ala- or HYNIC-Aoc- served as lead compounds with excellent characteristics. Yet, in view of the high tolerance of melanoma to ionizing radiation requiring a very high accumulation of

radionuclide in tumor lesions and hence high doses of radiopharmaceutical, the rate of MSH-mediated tumor uptake and retention of radionuclides by the tumor should first be further enhanced before larger clinical studies are started. We believe that it is less important to test too many different radionuclides with the same peptides and in the same experimental setting as there are more important open questions to solve at present: (1) the development of targeting systems with which the radionuclides are more rapidly and extensively internalized into tumor cells; (2) a better understanding of MC1R regulation in melanoma *in vivo* in order to find the most efficient targeting conditions; (3) the employment of PDOX models for selecting the most suitable radiopapetides; and (4) the study of appearance of α-MSH antibodies in the circulation under specific pathophysiological conditions. Such antibodies could scavange MSH radiopharmaceuticals, thus reducing the efficiency of any therapy. Once these and other open questions are resolved, a clinical study with the then most appropriate MSH radiocompound may lead to a real breakthrough in clinical melanoma targeting [161].

MBPs labeled with therapeutic radionuclides present an alternative to MSH radiopeptides, particularly in those situations where MC1R expression is low and where melanoma tumors are well melanized. However, the optimal peptide is not yet defined that exhibits minimal non-specific tissue uptake and long retention in the tumor lesion. Yet, MBPs are promising candidates for melanoma therapy warranting further development.

Research on MSH-photosensitizer constructs has only recently been started and therefore few data are available at this time. Nevertheless, as PDT has a great potential, MSH-photosensitizer conjugates may receive increased attention in the next few years. In particular, the development of more sophisticated light sources for precisely localized activation in the skin and other organs and the future availability of optimized peptide-photosensitizer conjugates will minimize or completely avoid collateral damage to the surrounding healthy cells.

LIST OF ABBREVIATIONS

ACTH	adrenocorticotropic hormone; adrenocorticotropin
Ahx	6-aminohexanoic acid
ALA	δ-aminolevulinic acid
Aoc	8-amino-octanoic acid
ASIP	agouti signaling peptide
BCC	basal cell carcinoma
βD3	β-defensin 3
BRAF	gene of the serine/threonine-protein kinase B-Raf
Bz-NCS	4-(isothiocyanate)benzyl
CBTE2A	4,11-*bis*(carboxymethyl)-1,4,8,11-tetraazabicyclo[6.6.2]hexadecane
CGRP	calcitonin gene-related peptide
CRH	corticotropin-releasing hormone; corticoliberin
CTLA-1	cyotoxic T-lymphocyte-associated antigen 1
DHP	2,3-dihydroxy-(2*S*)-propyl
DOTA	1,4,7,10-tetraazacyclododecane-1,4,7,10-tetraacetic acid
DOTATOC	DOTA-octreotide
DTPA	diethylenetriaminepentaacetic acid
EDDA	ethylenediamine-*N,N'*-diacetic acid

Gal	galactosyl
HPPH	2-[1-hexyloxyethyl]-2-devinyl pyropheophorbide-a
HYNIC	hydrazinonicotinic acid
IBA	iodobenzoate
IR	infrared
LED	light emitting diode
mAb	monoclonal antibody
MAG2	mercaptoacetylglycylglycyl
MAG3	mercaptoacetylglycylglycylglycyl
MAPK	mitogen-activated protein kinase
MBP	melanin-binding peptide
MCR1	melanocortin receptor 1
MRPT	melanin-binding peptide radiation therapy
MSH	melanocyte-stimulating hormone; melanotropin
NAP-amide	[Nle^4,Asp^5,*D*-Phe^7]-α-MSH$_{4-11}$
NDP-MSH	[Nle^4,*D*-Phe^7]-α-MSH
NOTA	1,4,7-triazacyclononane-1,4,7-triacetic acid
NPY	neuropeptide Y
PD-1	programmed cell death 1 receptor
PDOX	patient-derived orthotopic xenograft
PDT	photodynamic therapy
PET	positron emission tomography
PNP3	*N,N-bis*(dimethoxypropylphosphinoethyl)-methoxyethylamine
PPIX	protoporphyrin IX
Pra	*L*-propargylglycine
PRRT	peptide receptor radioaction therapy
Pz^1	*N*-{5-(*t*-butyl)isoxazol-3-yl}-2-{4-[5-(1-methyl-1H-pyrazol-4-yl)-1H-benzo[d]imidazol-1-yl]phenyl}-acetamide
Pz^4	4-{*N*-[2-(4-(2-carboxyethyl)-3,5-dimethyl-1*H*-pyrazol-1-yl)-ethyl], *N*-[(2-amino)ethyl]}amino-butanoic acid
RIT	radioimmunotherapy
SCC	squamous cell carcinoma
SFB	succinimidyl-4-fluorobenzoate
SPECT	single-photon emission computed tomography
Tyr(P)	phosphotyrosine
UV	ultraviolet
VIP	vasointestinal peptide

CONFLICT OF INTEREST

The authors declare no conflict of interest.

ACKNOWLEDGEMENTS

A.N.E. thanks the Swiss National Science Foundation and the Swiss Cancer League for financial support. B.R., M.B.Q., and P.L.B. thank the Joint Council Office, A* STAR, Singapore for grant no. 1234h00019. The authors thank Prof. Thomas P. Quinn, University of Missouri, Columbia MO, for generously providing the original of Figure 9.

REFERENCES

[1] Slominski, A.T.; Wortsman, J. Neuroendocrinology of the skin. *Endocr. Rev.*, **2000**, *21*(5), 457–487.

[2] Slominski, A.T.; Zmijewski, M.A.; Skobowiat, C.; Zbytek, B.; Slominski, R.M.; Steketee, J.D. Sensing the environment: Regulation of local and global homeostasis by the skin neuroendocrine system. *Adv. Anat. Embryol. Cell Biol.*, **2012**, *212*, 1–115.

[3] Reddy, B.; Jow, T.; Hantash, B.M. Bioactive oligopeptides in dermatology: Part I. *Exp. Dermatol.*, **2012**, *21*(8), 563–568.

[4] Reddy, B.; Jow, T.; Hantash, B.M. Bioactive oligopeptides in dermatology: Part II. *Exp. Dermatol.*, **2012**, *21*(8), 569–575.

[5] Hata, T.R.; Gallo, R.L. Antimicrobial peptides, skin infections, and atopic dermatitis. *Semin. Cutan. Med. Surg.*, **2008**, *27*(2), 144–150.

[6] Wiesner, J.; Vilcinskas, A. Antimicrobial peptides: the ancient arm of the human immune system. *Virulence*, **2010**, *1*(5), 440–464.

[7] Wang, G. Human antimicrobial peptides and proteins. *Pharmaceuticals*, **2014**, *7*(5), 545–594.

[8] Dutta, P.; Das, S. Mammalian antimicrobial peptides: promising therapeutic targets against infection and chronic inflammation. *Curr. Top. Med. Chem.*, **2016**, *16*(1), 99–129.

[9] Takahashi, T.; Gallo, R.L. The critical and multifunctional roles of antimicrobial peptides in dermatology. *Dermatol. Clin.*, **2017**, *35*(1), 39–50.

[10] Conlon, J.M. Host-defense peptides of the skin with therapeutic potential: from hagfish to human. *Peptides*, **2015**, *67*, 29–38.

[11] Schauer E.; Trautinger F.; Köck, A.; Schwarz, A.; Bhardwaj, R.; Simon, M.; Ansel, J.C.; Schwarz, T.; Luger, T.A. Proopiomelanocortin-derived peptides are synthesized and released by human keratinocytes. *J. Clin. Invest.*, **1994**, *93*(5), 2258–2262.

[12] Slominski, A.T.; Tobin, D.J.; Shibahara, S.; Wortsman, J. Melanin pigmentation in mammalian skin and its hormonal regulation. *Physiol. Rev.*, **2004**, *84*(4), 1155–1228.

[13] Slominski, A.T.; Wortsman, J.; Luger, T.; Paus, R.; Solomon, S. Corticotropin releasing hormone and proopiomelanocortin involvement in the cutaneous response to stress. *Physiol. Rev.*, **2000**, *80*(3), 979–1020.

[14] Slominski, A.T.; Zmijewski, M.A.; Zbytek, B.; Tobin, D.J.; Theoharides, T.C.; Rivier, J. Key role of CRF in the skin stress response system. *Endocr. Rev.*, **2013**, *34*(6), 827–884.

[15] Bigliardi, P.L.; Bigliardi-Qi, M.; Büchner, S.; Rufli, T. Expression of μ-opiate receptor in human epidermis and keratinocytes. *J. Invest. Dermatol.*, **1998**, *111*(2), 297–301.

[16] Bigliardi-Qi, M.; Bigliardi, P.L.; Eberle, A.N.; Büchner, S.; Rufli, T. β-Endorphin stimulates cytokeratin 16 expression and downregulates μ-opiate receptor expression in human epidermis. *J. Invest. Dermatol.*, **2000**, *114*(3), 527–532.

[17] Slominski, A.T.; Zmijewski, M.A.; Zbytek, B.; Brozyna, A.A.; Granese, J.; Pisarchik, A.; Szczesniewski, A.; Tobin, D.J. Regulated proenkephlin expression in human skin and cultured skin cells. *J. Invest. Dermatol.*, **2011**, *131*(3), 613–622.

[18] Bigliardi, P.L.; Dancik, Y.; Neumann, C.; Bigliardi-Qi, M. Opioids and skin homeostasis, regeneration and ageing – What's the evidence? Exp. Dermatol., 2016, 25(8), 586–591.

[19] N'Diaye A.; Gannesen, A.; Borrel, V.; Maillot, O.; Enault, J.; Racine, P.-J.; Plakunov, V.; Chevalier, S.; Lesouhaitier, O.; Feuilloley, M.G.J. Substance P and calcitonin gene-related peptide: Key regulators of cutaneous microbiota homeostasis. *Front. Endocrinol.*, **2017**, *8*, 15. doi: 10.3389/fendo.2017.00015.

[20] Wallengren, J. Vasoactive peptides in the skin. *J. Investig. Dermatol. Symp. Proc.*, **1997**, *2*(1), 49–56.

[21] Heppeler, A.; Froidevaux, S.; Eberle, A.N.; Mäcke, H.R. Receptor targeting for tumor localization and therapy with radiopeptides. *Curr. Med. Chem.*, **2000**, *7*(9), 971–994.

[22] Conlon, J.M.; Mechkarska, M.; Lukic, M.L.; Flatt, P.R. Potential therapeutic applications of multifunctional host-defense peptides from frog skin as anti-cancer, anti-vial, immunomodulatory and anti-diabetic agents. *Peptides*, **2014**, *57*, 67–77.

[23] Mohan, S.V.; Chang, A.L. Advanced basal cell carcinoma: epidemiology and therapeutic innovations. *Curr. Dermatol. Rep*., **2014**, *3*, 40–45.

[24] Green, A.C.; Olsen, C.M. Cutaneous squamous cell carcinoma: an epidemiological review. *Br. J. Dermatol.*, **2017**, doi: 10.1111/bjd.15324.

[25] Tsao, H.; Fukunaga-Kalabis, M.; Herlyn, M. Recent advances in melanoma and melanocyte biology. *J. Invest. Dermatol.*, **2017**, *137*(3), 557–560.

[26] Ansai, S.I. Topics in histopathology of sweat gland and sebaceous neoplasms. *J. Dermatol.*, **2017**, *44*(3), 315–326.

[27] Park, J.H.; Lee, D.Y.; Kim, N. Nail neoplasms. *J. Dermatol.*, **2017**, *44*(3), 279–287.

[28] Takai, T. Advances in histopathological diagnosis of keratoacanthoma. *J. Dermatol.*, **2017**, *44*(3), 304–314.

[29] Schadendorf, D.; Lebbé, C.; Zur Hausen, A.; Avril, M.F.; Hariharan, S.; Bharmal, M.; Becker, J.C. Merkel cell carcinoma: epidemiology, prognosis, therapy and unmet medical needs. *Eur. J. Cancer*, **2017**, *71*, 53–69.

[30] Gallagher, R.P.; Hill, G.B.; Bajdik, C.D.; Fincham, S.; Coldman, A.J.; McLean, D.I.; Threlfall, W.J. Sunlight exposure, pigmentary factors, and risk of nonmelanocytic skin cancer. I. Basal cell carcinoma. *Arch. Dermatol.*, **1995**, *131*(2), 157−163.

[31] Lewin, J.M.; Carucci, J.A. Advances in the management of basal cell carcinoma. *F1000Prime Rep.*, **2015**, *7*, 53. DOI: 10.12703/P7-53

[32] Gallagher, R.P.; Hill, G.B.; Bajdik, C.D.; Coldman, A.J.; Fincham, S.; McLean, D.I.; Threlfall, W.J. Sunlight exposure, pigmentary factors, and risk of nonmelanocytic skin cancer. II. Squamous cell carcinoma. *Arch. Dermatol.*, **1995**, *131*(2), 164−169.

[33] Stratigos, A.; Garbe, C.; Lebbe, C.; Malvehy, J.; del Marmol, V.; Pehamberger, H.; Peris, K.; Becker, J.C.; Zalaudek, I.; Saiag, P.; Middleton, M.R.; Bastholt, L.; Testori, A.; Grob, J.J. Diagnosis and treatment of invasive squamous cell carcinoma of the skin: European consensus-based interdisciplinary guideline. *Eur. J. Cancer*, **2015**, *51*(14), 1989−2007.

[34] Do, N.; Weindl, G.; Grohmann, L.; Salwiczek, M.; Koksch, B.; Korting, H.C.; Schäfer-Korting, M. Cationic membrane-active peptides – anticancer and antifungal activity as well as penetration into human skin. *Exp. Dermatol.*, **2014**, *23*(5), 326−331.

[35] Kanazawa, T.; Misawa, K.; Misawa, Y.; Uehara, T.; Fukushima, H.; Kusaka, G.; Maruta, M.; Carey, T.E. G-protein-coupled receptors: next generation therapeutic targets in head and neck cancer? *Toxins*, **2015**, *7*(8), 2959−2984.

[36] Ferlay, J.; Steliarova-Foucher, E.; Lortet-Tieulent, J.; Rosso, S.; Coebergh, J.W.W.; Comber, H.; Forman, D.; Bray, F. Cancer incidence and mortality patterns in Europe: estimates for 40 countries in 2012. *Eur. J. Cancer*, **2013**, *49*(6), 1374−1403.

[37] Howlader, N.; Noone, A.M.; Krapcho, M.; Miller, D.; Bishop, K.; Altekruse, S.F.; Kosary, C.L.; Yu, M.; Ruhl, J.; Tatalovich, Z.; Mariotto, A.; Lewis, D.R.; Chen, H.S.; Feuer, E.J.; Cronin, K.A. SEER Cancer Statistics Review, 1975−2013, National Cancer Institute. Bethesda, MD, http://seer.cancer.gov/csr/1975_2013/, based on November 2015 SEER data submission, posted to the SEER web site, April 2016.

[38] Gallagher, R.P.; McLean, D.I. The epidemiology of acquired melanocytic nevi. A brief review. *Dermatol. Clinic*, **1995**, *13*(3), 595−603.

[39] Lian, C.G.; Mihm, M.C. Skin Cancer. In: *World Cancer Report*; Stewart, B.W.; Wild, C.P., Eds.; International Agency for Research on Cancer: Lyon, France, **2014**; pp. 495−502.

[40] Tan, W.W. Malignant melanoma treatment and management. *Medscape*, **2016**. http://emedicine.medscape.com/article/280245-treatment - d1

[41] Raigani, S.; Cohen, S.; Boland, G.M. The role of surgery for melanoma in an era of effective systemic therapy. *Curr. Oncol. Rep.*, **2017**, *19*, 17. DOI: 10.1007/s11912-017-0575-8

[42] Bilsland, A.E.; Spiliopoulou, P.; Evans, T.R. Virotherapy: Cancer gene therapy at last? *F1000Research*, **2016**, *5* (F1000 Faculty Rev), 2105. DOI: 10.12688/f1000research.8211.1

[43] Kudchadkar, R.R.; Smalley, K.S.M.; Glass, L.F.; Trimble, J.S.; Sondak, V.K. Targeted therapy in melanoma. *Clin. Dermatol.*, **2013**, *31*(2), 200–208.

[44] Acosta, A.M.; Kadkol, S.H.S. Mitogen-activated protein kinase signaling in cutaneous melanoma. *Arch. Pathol. Lab. Med.*, **2016**, *140*(11), 1290–1296.

[45] Amaral, T.; Sinnberg, T.; Meier, F.; Krepler, C.; Levesque, M.; Niessner, H.; Garbe, C. MAPK pathway in melanoma part I. Activation and primary resistance mechanisms to BRAF inhibition. *Eur. J. Cancer*, **2017**, *73*, 85–92.

[46] Amaral, T.; Sinnberg, T.; Meier, F.; Krepler, C.; Levesque, M.; Niessner, H.; Garbe, C. MAPK pathway in melanoma part II. Secondary and adaptive resistance mechanisms to BRAF inhibition. *Eur. J. Cancer*, **2017**, *73*, 93–101.

[47] Eberle, A.N. *The Melanotropins; Chemistry, Physiology and Mechanisms of Action*; Karger: Basel, **1988**.

[48] Lahiri, K.; Chatterjee, M.; Sarkar, R. *Pigmentary Disorders: A Comprehensive Compendium*. JP Medical: London, **2014**.

[49] Siegrist, W.; Stutz, S.; Girard, J.; Eberle, A.N. Binding assay for the study of melanoma cell MSH receptors. In: *Progress in Cancer Research and Therapy*; Bresciani, F., King, R.J.B., Lippman, M.E., Raynaud, J.-P., Eds.; Raven Press: New York, **1988**; Vol. *35: Hormones and Cancer*, pp. 314–317.

[50] Ghanem, G.E.; Comunale, G.; Libert, A.; Vercammen-Grandjean, A.; Lejeune, F.J. Evidence for α-melanocyte-stimulating hormone (α-MSH) receptors on human malignant melanoma cells. *Int. J. Cancer*, **1988**, *41*(2), 248–255.

[51] Siegrist, W.; Solca, F.; Stutz, S.; Giuffrè, L.; Carrel, S.; Girard, J.; Eberle, A.N. Characterization of receptors for α-melanocyte-stimulating hormone on human melanoma cells. *Cancer Res.*, **1989**, *49*(22), 6352–6358.

[52] Scimonelli, T.; Eberle, A.N. Photoaffinity labeling of melanoma cell MSH receptors. *FEBS Lett.*, **1987**, *226*(1), 134–138.

[53] Solca, F.; Siegrist, W.; Drozdz, R.; Girard, J.; Eberle, A.N. The receptor for α-melanotropin of mouse and human melanoma cells. Application of a potent α-melanotropin photoaffinity label. *J. Biol. Chem.*, **1989**, *264*(24), 14277–14281.

[54] Eberle, A.N.; de Graan, P.N.E.; Scimonelli, T.; Solca, F. Photoaffinity labeling of melanocyte-stimulating hormone receptors. *Pharmacol. Ther.*, **1989**, *44*(1), 63–83.

[55] Mountjoy, K.G.; Robbins, L.S.; Mortrud, M.T., Cone, R.D. The cloning of a family of genes that encode the melanocortin receptors. *Science*, **1992**, *257*(5074), 1248–1251.

[56] Chhajlani, V.; Wikberg, J.E. Molecular cloning and expression of the human melanocyte stimulating hormone receptor cDNA. *FEBS Lett.*, **1992**, *309*(3), 417–420.

[57] De Luca, M.; Siegrist, W.; Bondanza, S.; Mathor, M.; Cancedda, R.; Eberle, A.N. α-Melanocyte stimulating hormone (α-MSH) stimulates normal human melanocyte growth by binding to high-affinity receptors. *J. Cell Sci.*, **1993**, *105*, 1079–1084.

[58] Eberle, A.N.; Siegrist, W.; Bagutti, C.; Chluba-de Tapia, J.; Solca, F.; Wikberg, J.E.S.; Chhajlani, V. Receptors for melanocyte-stimulating hormone on melanoma cells. *Ann. N.Y. Acad. Sci.*, **1993**, *680*, 320–341.

[59] Siegrist, W.; Stutz, S.; Eberle, A.N. Homologous and heterologous regulation of α-melanocyte-stimulating hormone receptors in human and mouse melanoma cell lines. *Cancer Res.*, **1994**, *54*(10), 2604–2610.

[60] Jiang, J.; Sharma, S.D.; Fink, J.L.; Hadley, M.E.; Hruby, V.J. Melanotropic peptide receptors: membrane markers of human melanoma cells. *Exp. Dermatol.*, **1996**, *5*(6), 325–333.

[61] Salazar-Onfray, F.; López, M.; Lundqvist, A.; Aguirre, A.; Escobar, A.; Serrano, A.; Korenblit, C.; Petersson, M.; Chhajlani, V.; Larsson, O.; Kiessling, R. Tissue distribution and differential expression of melanocortin 1 receptor, a malignant melanoma marker. *Br. J. Cancer*, **2002**, *87*(4), 414–422.

[62] Sawyer, T.K.; Sanfilippo, P.J.; Hruby, V.J.; Engel, M.H.; Heward, C.B.; Burnett, J.B.; Hadley, M.E. 4-Norleucine, 7-D-phenylalanine-α-melanocyte-stimulating hormone: a highly potent α-melanotropin with ultralong biological activity. *Proc. Natl. Acad. Sci. USA*, **1980**, *77*(10), 5754–5758.

[63] Hadely, M.E.; Dorr, R.T. Melanocortin peptide therapeutics: historical milestones, clinical studies and commercialization. *Peptides*, **2006**, *27*(4), 921–930.

[64] Koikov, L.N.; Ebetino, F.H.; Solinsky, M.G.; Cross-Doersen, D.; Knittel, J.J. Sub-nanomolar hMC1R agonists by end-capping of the melanocortin tetrapeptide His-*D*-Phe-Arg-Trp-NH_2. *Bioorg. Med. Chem. Lett.*, **2003**, *13*(16), 2647–2650.

[65] Abdel-Malek, Z.A.; Ruwe, A.; Kavanagh-Stamer, R.; Kadekaro, A.L.; Swope, V.; Haskell-Luevano, C.; Koikov, L.; Knittel, J.J. α-MSH tripeptide analogs activate the melanocortin 1 receptor and reduce UV-induced DNA damage in human melanocytes. *Pigment Cell Melanoma Res.*, **2009**, *22*(5), 635–644.

[66] Habbema, L.; Halk, A.B.; Neumann, M.; Bergman, W. Risks of unregulated use of α-melanocyte-stimulating hormone analogues: a review. *Int. J. Dermatol.*, **2017**. [Epub ahead of print]. DOI: 10.1111/ijd.13585

[67] Lu, D.; Willard, D.; Patel, I.R.; Kadwell, S.; Overton, L.; Kost, T.; Luther, M.; Chen, W.; Woychik, R.P.; Wilkison, W.O. Agouti protein is an antagonist of the melanocyte-stimulating-hormone receptor. *Nature*, **1994**, *371*(6500), 799–802.

[68] Kansal, R.G.; McCravy, M.S., Basham, J.H.; Earl, J.A.; McMurray, S.L.; Stamer, C.J.; Whitt, M.A.; Albritton, L.M. Inhibition of melanocortin 1 receptor slows melanoma growth, reduces tumor heterogeneity and increases survival. *Oncotarget*, **2016**, *7*(18), 26331–26345.

[69] Landi, M.T.; Bauer, J.; Pfeiffer, R.M.; Elder, D.E.; Hulley, B.; Minghetti, P.; Calista, D.; Kanetsky, P.A.; Pinkel, D.; Bastian, B.C. MC1R germline variants confer risk for BRAF-mutant melanoma. *Science*, **2006**, *313*(5786), 521–522.

[70] Eberle, A.N.; Froidevaux, S. Radiolabeled α-melanocyte-stimulating hormone analogs for receptor-mediated targeting of melanoma: from tritium to indium. *J. Mol. Recognit.*, **2003**, *16*(5), 248–254.

[71] Bard, D.R.; Knight, C.G.; Page-Thomas, D.P. A chelating derivative of α-melanocyte stimulating hormone as potential imaging agent for malignant melanoma. *Br. J. Cancer*, **1990**, *62*(6), 919–922.

[72] Bard, D.R.; Knight, C.G.; Page-Thomas, D.P. Targeting of a chelating derivative of a short-chain analogue of α-melanocyte stimulating hormone to Cloudman S91 melanomas. *Biochem. Soc. Trans.*, **1990**, *18*(5), 882–883.

[73] Wraight, E.P.; Bard, D.R.; Maughan, T.S.; Knight, C.G.; Page-Thomas, D.P. The use of a chelating derivative of α-melanocyte stimulating hormone for the clinical imaging of malignant melanoma. *Br. J. Radiol.*, **1992**, *65*(770), 112–118.

[74] Bagutti, C.; Stolz, B.; Albert, R.; Bruns, C.; Pless, J.; Eberle, A.N. [^{111}In]-DTPA-labeled analogues of α-melanocyte-stimulating hormone for melanoma targeting: receptor binding in vitro and in vivo. *Int. J. Cancer*, **1994**, *58*(5), 749–755.

[75] Bagutti, C.; Oestreicher, M.; Siegrist, W.; Oberholzer, M.; Eberle, A.N. α-MSH receptor autoradiography on mouse and human melanoma tissue sections and biopsies. *J. Recept. Signal Transduct. Res.*, **1995**, *15*(1–4), 427–442.

[76] Reith, M.E.; Neidle, A. Breakdown and fate of ACTH and MSH. *Pharmacol. Ther.*, **1981**, *12*(3), 449–461.

[77] Eberle, A.N. Proopiomelanocortin and the melanocortin peptides. In: *The Melanocortin Receptors*; Cone, R.D., Ed.; Humana Press: Totowa NJ, **2000**; pp. 3–67.

[78] Holder, J.R.; Haskell-Luevano, C. Melanocortin ligands: 30 years of structure-activity relationship (SAR) studies. *Med. Res. Rev.*, **2004**, *24*(3), 325-356.

[79] Froidevaux, S.; Calame-Christe, M.; Schuhmacher, J.; Tanner, H.; Saffrich, R.; Henze, M.; Eberle, A.N. A gallium-labeled DOTA-α-melanocyte-stimulating hormone analog for PET imaging of melanoma metastases. *J. Nucl. Med.*, **2004**, *45*(1), 116–123.

[80] Wolf Horrell, E.M.; Boulanger, M.C.; D'Orazio, J.A. Melanocortin 1 receptor: Structure, function and regulation. *Front. Genet.*, **2016**, *7:95*. DOI: 10.3389/fgene.2016.00095

[81] McNulty, J.C.; Jackson, P.J.; Thompson, D.A.; Chai, B.; Gantz, I.; Barsh, G.S.; Dawson, P.E.; Millhauser, G.L. Structures of the agouti signaling protein. *J. Mol. Biol.*, **2005**, *346*(4), 1059–1070.

[82] Dholpe, V.; Krukemeyer, A.; Ramamoorthy, A. The human β-defensin-3, an antibacterial peptide with multiple biological functions. *Biochim. Biophys. Acta*, **2006**, *1758*(9), 1499–1512.

[83] Eberle, A.N.; Bódi, J.; Orosz, G.; Süli-Vargha, H.; Jäggin, V.; Zumsteg, U. Antagonist and agonist activities of the mouse agouti protein fragment (91-131) at the melanocortin-1 receptor. *J. Recept Signal Transduct. Res.*, **2001**, *21*(1), 25–45.

[84] Cai, M.; Stankova, M.; Muthu, D.; Mayorov, A.; Yang, Z.; Trivedi, D.; Cabello, C.; Hruby, V.J. An unusual conformation of MSH analogues leads to a selective human melanocortin 1 receptor antagonist for targeting melanoma cells. *Biochemistry*, **2013**, *52*(4), 752–764.

[85] Nosanchuk, J.D.; Valadon, P.; Feldmesser, M.; Casadevall, A. Melanization of *Cryptococcus neoformans* in murine infection. *Mol. Cell. Biol.*, **1999**, *19*(1), 745–750.

[86] Norain, A.; Dadachova, E. Targeted radionuclide therapy of melanoma. *Semin. Nucl. Med.*, **2016**, *46*(3), 250–259.

[87] Hantash, B.M.; Jimenez, F. A split-face, double-blind, randomized and placebo-controlled pilot evaluation of a novel oligopeptide for the treatment of recalcitrant melasma. *J. Drug Dermatol.*, **2009**, *8*(8), 732–735.

[88] Siegrist, W.; Eberle, A.N. Homologous regulation of the MSH receptor in melanoma cells. *J. Recept. Res.*, **1993**, *13*(1–4), 263–281.

[89] Sánchez-Laorden, B.L.; Jiménez-Cervantes, C.; Garcia-Borrón, J.C. Regulation of human melanocortin 1 receptor signaling and trafficking by Thr-308 and Ser-316 and its alteration in variant alleles associated with red hair and skin cancer. *J. Biol. Chem.*, **2007**, *282*(5), 3241–3251.

[90] Pavlos, N.J.; Friedman, P.A. GPCR signaling and trafficking: the long and short of it. *Trends Endocrinol. Metab.*, **2017**, *28*(3), 213–226.

[91] Wang, M.; Caruano, A.L.; Lewis, M.R.; Meyer, L.A.; Vander Waal, R.P.; Anderson, C.J. Subcellular localization of radiolabeled somatostatin analogues: implications for targeted radiotherapy of cancer. *Cancer Res.*, **2003**, *63*(20), 6864–6869.

[92] Eberle, A.N.; Mild, G. Receptor-mediated tumor targeting with radiopeptides. Part I. General principles and methods. *J. Recept. Signal Transd.*, **2009**, *29*(1), 1–37.

[93] Deshpande, S.V.; DeNardo, S.J.; Kukis, D.L.; Moi, M.K.; McCall, M.J.; DeNardo, G.L.; Meares, C.F. Yttrium-90-labeled monoclonal antibody for therapy: labeling by a new macrocyclic bifunctional chelating agent. *J. Nucl. Med.*, **1990**, *31*(4), 473–479.

[94] Brechbiel, M.W.; Gansow, O.A. Synthesis of C-functionalized trans-cyclohexyl-diethylenetriaminepenta-acetic acids for labeling of monoclonal antibodies with the bismuth-212 α-particle emitter. *J. Chem. Soc. Perkin 1*, **1992**, 1173–1178.

[95] Wei, L.; Zhang, X.; Gallazzi, F.; Miao, Y.; Jin, X.; Brechbiel, M.W.; Xu, H.; Clifford, T.; Welch, M.J., Lewis, J.S.; Quinn, T.P. Melanoma imaging using ^{111}In-, ^{86}Y- and ^{68}Ga-labeled CHX-A"-Re[Arg^{11}]CCMSH. *Nucl. Med. Biol.*, **2009**, *36*(4), 345–354.

[96] Cantorias, M.V.; Figueroa, S.D.; Quinn, T.P.; Lever, J.R.; Hoffmann, T.J.; Watkinson, L.D.; Carmack, T.L.; Cutler, C.S. Development of high-specific activity ^{68}Ga-

labeled DOTA-rhenium-cyclized α-MSH peptide analog to target MC1 receptors overexpressed by melanoma tumors. *Nucl. Med. Biol.*, **2009**, *36*(5), 505–513.

[97] Wei, L.; Butcher, C.; Miao, Y.; Gallazzi, F.; Quinn, T.P.; Welch, M.J.; Lewis, J.S. Synthesis and biologic evaluation of ^{64}Cu-labeled rhenium-cyclized α-MSH peptide analog using a cross-bridged cyclam chelator. *J. Nucl. Med.*, **2007**, *48*(1), 64–72.

[98] Zhang, X.; Yue, Z.; Lu, B.Y.; Vazquez-Flores, G.J.; Yuen, J.; Figueroa, S.D.; Gallazzi, F.; Cutler, C.; Quinn, T.P.; Lacy, J.L. Copper-62 labeled ReCCMSH peptide analogs for melanoma PET imaging. *Curr. Radiopharm.*, **2012**, *5*(4), 329–335.

[99] Gao, F.; Sihver, W.; Jurischka, C.; Bergmann, R.; Haase-Kohn, C.; Mosch, B.; Steinbach, J.; Carta, D.; Bolzati, C.; Calderan, A.; Pietzsch, J.; Pietzsch, H.-J. Radiopharmacological characterization of ^{64}Cu-labeled α-MSH analogs for potential use in imaging of malignant melanoma. *Amino Acids*, **2016**, *48*(3), 833–847.

[100] Liu, G.; Hnatowich, D.J. Labeling biomolecules with radiorhenium – a review of the bifunctional chelators. *Anticancer Agents Med. Chem.*, **2007**, *7*(3), 367–377.

[101] Giblin, M.F.; Wang, N.; Hoffman, T.J.; Jurisson, S.S.; Quinn, T.P. Design and characterization of α-melanotropin peptide analogs cyclized through rhenium and technetium metal coordination. *Proc. Natl. Acad. Sci. USA*, **1998**, *95*(22), 12814–12818.

[102] Giblin, M.F.; Jurisson, S.S.; Quinn, T.P. Synthesis and characterization of rhenium-complexed α-melanotropin analogs. *Bioconjug. Chem.*, **1997**, *8*(3), 347–353.

[103] Chen, J.; Giblin, M.F.; Wang, N.; Jurisson, S.S.; Quinn, T.P. In vivo evaluation of ^{99m}Tc/^{188}Re-labeled linear α-melanocyte stimulating hormone analogs for specific melanoma targeting. *Nucl. Med. Biol.*, **1999**, *26*(6), 687–693.

[104] Zhang, X.; Teixeira, V.; Porcal, W.; Cabral, P.; Gambini, J.P.; Fernández, M.; Quinn, T.P. [^{99m}Tc(CO)$_3$]$^+$ and [^{99m}TcO$_2$]$^+$ radiolabeled cyclic melanotropin peptides for melanoma SPECT imaging. *Curr. Radiopharm.*, **2014**, *7*(1), 63–74.

[105] Garcia, M.F.; Zhang, X.; Gallazzi, F.; Fernández, M.; Moreno, M.; Gambini, J.P.; Porcal, W.; Cabral, P.; Quinn, T.P. Evaluation of tricine and EDDA as co-ligands for ^{99m}Tc-labeled HYNIC-MSH analogs for melanoma imaging. *Anticancer Agents Med. Chem.*, **2015**, *15*(1), 122–130.

[106] Shamshirian, D.; Erfani, M.; Beiki, D.; Hajiramazanali, M.; Fallahi, B. A ^{99m}Tc-trycine-HYNIC-labeled peptide targeting the melanocortin-1 receptor for melanoma imaging. *Iran J. Pharm. Res.*, **2016**, *15*(3), 349–360.

[107] Teixeira, V.; Fernández, M.; Oddone, N.; Zhang, X.; Gallazzi, F.; Cerecetto, H.; Gambini, J.P.; Porcal, W.; Cabral, P.; Quinn, T.P. The effect of hexanoic acid linker insertion on the pharmacokinetics and tumor targeting properties of the melanoma imaging agent ^{99m}Tc-HYNIC-cycMSH. *Anticancer Agents Med. Chem.*, **2016**, [Epub ahead of print]. DOI: 10.2174/1871520616666161206144414.

[108] Carta, D.; Salvarese, N.; Morellato, N.; Gao, F.; Sihver, W.; Pietzsch, H.J.; Biondi, B.; Ruzza, P.; Refosco, F.; Carpanese, D.; Rosato, A.; Bolzati, C. Melanoma targeting with [^{99m}Tc(N)(PNP3)]-labeled α-melanocyte stimulating hormone peptide analogs: Effects of cyclization on the radiopharmaceutical properties. *Nucl. Med. Biol.*, **2016**, *43*(12), 788–801.

[109] Bard, D.R. An improved imaging agent for malignant melanoma, based on [Nle^4,*D*-Phe^7]α-melanocyte stimulating hormone. *Nucl. Med. Commun*., **1995**, *16*(10), 860–866.

[110] Froidevaux, S.; Calame-Christe, M.; Tanner, H.; Sumanovski, L.; Eberle, A.N. A novel DOTA-α-melanocyte-stimulating hormone analog for metastatic melanoma diagnosis. *J. Nucl. Med.*, **2002**, *43*(12), 1699–1706.

[111] Hammond, P.J.; Wade, A.F.; Gwilliam, M.E.; Peters, A.M.; Myers, M.J.; Gilbey, S.G.; Blum, S.R.; Calam, J. Amino acid infusion blocks renal tubular uptake of an indium-labelled somatostatin analogue. *Br. J. Cancer*, **1993**, *67*(6), 1437–1439.

[112] Cheng, Z.; Zhang, L.; Graves, E.; Xiong, Z.; Dandekar, M.; Chen, X.; Gambhir, S.S. Small-animal PET of melanocortin 1 receptor expression using a ^{18}F-labeled α-melanocyte-stimulating hormone analog. *J. Nucl. Med.*, **2007**, *48*(6), 987–994.

[113] Ren, G.; Liu, Z.; Miao, Z.; Liu, H.; Subbarayan, M.; Chin, F.T.; Zhang, L.; Gambhir, S.S.; Cheng, Z. PET of malignant melanoma using ^{18}F-labeled metallopeptides. *J. Nucl. Med.*, **2009**, *50*(11), 1865–1872.

[114] Froidevaux, S.; Calame-Christe, M.; Tanner, H.; Eberle, A.N. Melanoma targeting with DOTA-α-melanocyte-stimulating hormone analogs: structural parameters affecting tumor uptake and kidney uptake. *J. Nucl. Med.*, **2005**, *46*(5), 887–895.

[115] Bapst, J.-P.; Froidevaux, S.; Calame, M.; Tanner, H.; Eberle, A.N. Dimeric DOTA-α-melanocyte-stimulating hormone analogs: synthesis and *in vivo* characteristics of radiopeptides with high *in vitro* activity. *J. Recept. Signal Transduct.*, **2007**, *27*(5–6), 383–409.

[116] Bapst, J.-P.; Calame, M.; Tanner, H.; Eberle, A.N. Glycosylated DOTA-α-melanocyte-stimulating hormone analogues for melanoma targeting: influence of the site of glycosylation on in vivo biodistribution. *Bioconjug. Chem.*, **2009**, *20*(5), 984–993.

[117] Bapst, J.-P.; Eberle, A.N. Receptor-mediated melanoma targeting with radiolabeled α-melanocyte-stimulating hormone: relevance of the net charge of the ligand. *Front. Endocrinol.*, **2017**, *8:93*. DOI: 10.3389/fendo.2017.00093.

[118] Sawyer, T.K.; Hruby, V.J.; Darman, P.S.; Hadley, M.E. [half-Cys^4,half-Cys^{10}]-α-melanocyte-stimulating hormone: a cyclic α-melanotropin exhibiting superagonist biological activity. *Proc. Natl. Acad. Sci. USA*, **1982**, *79*(6), 1751–1755.

[119] Cody, W.L.; Wilkes, B.C.; Muska, B.J.; Hruby, V.J.; de L. Castrucci, A.M.; Hadley, M.E. Cyclic melanotropins. 5. Importance of the C-terminal tripeptide (Lys-Pro-Val). *J. Med. Chem.*, **1984**, *27*(9), 1186–1190.

[120] Cai, M.; Hruby, V.J. Design of cyclized selective melanotropins. *Biopolymers*, **2016**, *106*(6), 876–883.

[121] Al-Obeidi, F.; Castrucci, A.M.; Hadley, M.E.; Hruby, V.J. Potent and prolonged acting cyclic lactam analogues of α-melanotropin: design based on molecular dynamics. *J. Med. Chem.*, **1989**, *32*(12), 2555–2561.

[122] Chen, J.; Cheng, Z.; Hoffman, T.J.; Jurisson, S.S.; Quinn, T.P. Melanoma-targeting properties of ^{99m}technetium-labeled cyclic α-melanomacyte-stimulating hormone peptide analogues. *Cancer Res.*, **2000**, *60*(20), 5649–5658.

[123] Miao, Y.; Owen, N.K.; Whitener, D.; Gallazzi, F.; Hoffman, T.J.; Quinn, T.P. In vivo evaluation of ^{188}Re-labeled α-melanocyte stimulating hormone peptide analogs for melanoma therapy. *Int. J. Cancer*, **2002**, *101*(5), 480–487.

[124] Miao, Y.; Whitener, D.; Feng, W.; Owen, N.K.; Chen, J.; Quinn, T.P. Evaluation of the human melanoma targeting properties of radiolabeled α-melanocyte stimulating hormone peptide analogues. *Bioconjug. Chem.*, **2003**, *14*(6), 1177–1184.

[125] Cheng, Z.; Chen, J.; Quinn, T.P.; Jurisson, S.S. Radioiodination of rhenium cyclized α-melanocyte-stimulating hormone resulting in enhanced radioactivity localization and retention in melanoma. *Cancer Res.*, **2004**, *64*(4), 1411–1418.

[126] Chen, J.; Cheng, Z.; Owen, N.K.; Hoffman, T.J.; Miao, Y.; Jurisson, S.S.; Quinn, T.P. Evaluation of an ^{111}In-DOTA-rhenium cyclized α-MSH analog: a novel cyclic-peptide analog with improved tumor-targeting properties. *J. Nucl. Med.*, **2001**, *42*(12), 1847–1855.

[127] Chen, J.; Cheng, Z.; Miao, Y.; Jurisson, S.S.; Quinn, T.P. α-Melanocyte-stimulating hormone peptide analogs labeled with technetium-99m and indium-111 for malignant melanoma targeting. *Cancer*, **2002**, *94*(4 Suppl.), 1196–1201.

[128] Cheng, Z.; Chen, J.; Miao, Y.; Owen, N.K.; Quinn, T.P.; Jurisson, S.S. Modification of the structure of a metallopeptide: synthesis and biological evaluation of ^{111}In-labeled DOTA-conjugated rhenium-cyclized α-MSH analogues. *J. Med. Chem.*, **2002**, *45*(14), 3048–3056.

[129] McQuade, P.; Miao, Y.; Yoo, J.; Quinn, T.P.; Welch, M.J.; Lewis, J.S. Imaging of melanoma using ^{64}Cu- and ^{86}Y-DOTA-ReCCMSH(Arg^{11}), a cyclized peptide analogue of α-MSH. *J. Med. Chem.*, **2005**, *48*(8), 2985–2992.

[130] Wei, L.; Miao, Y.; Gallazzi, F.; Quinn, T.P.; Welch, M.J.; Vavere, A.L.; Lewis, J.S. Ga-68 labeled DOTA-rhenium cyclized α-MSH analog for imaging of malignant melanoma. *Nucl. Med. Biol.*, **2007**, *34*(8), 945–953.

[131] Miao, Y.; Benwell, K.; Quinn, T.P. ^{99m}Tc- and ^{111}In-labeled α-melanocyte-stimulating hormone peptides as imaging probes for primary and pulmonary metastatic melanoma detection. *J. Nucl. Med.*, **2007**, *48*(1), 73–80.

[132] Miao, Y.; Figueroa, S.D.; Fisher, D.R.; Moore, H.A.; Testa, R.F.; Hoffman, T.J., Quinn, T.P. ^{203}Pb-labeled α-melanocyte-stimulating hormone peptide as an imaging probe for melanoma detection. *J. Nucl. Med.*, **2008**, *49*(5), 823–829.

[133] Yang, J.; Liu, L.; Miao, Y. Effects of the Arg-Pro and Gly-Gly-Nle moieties on melanocortin-1 receptor binding affinities of α-MSH peptides. *ACS Med. Chem. Lett.*, **2013**, *4*(10), 1000–1004.

[134] Raposinho, P.D.; Xavier, C.; Correia, J.D.G.; Falcão, S.; Gomes, P.; Santos, I. Melanoma targeting with α-melanocyte stimulating hormone analogs labeled with *fac*-[^{99m}Tc(CO)$_3$]$^+$: effect of cyclization on tumor-seeking properties. *J. Biol. Inorg. Chem.*, **2008**, *13*(3), 449–459.

[135] Miao, Y.; Gallazzi, F.; Guo, H.; Quinn, T.P. ^{111}In-labeled lactam bridge-cyclized α-melanocyte stimulating hormone peptide analogues for melanoma imaging. *Bioconjug. Chem.*, **2008**, *19*(2), 539–547.

[136] Guo, H.; Shenoy, N.; Gershman, B.M.; Yang, J.; Sklar, L.A.; Miao, Y. Metastatic melanoma imaging with an ^{111}In-labeled lactam bridge-cyclized α-melanocyte-stimulating hormone peptide. *Nucl. Med. Biol.*, **2009**, *36*(3), 267–276.

[137] Guo, H.; Yang, J.; Shenoy, N.; Miao, Y. Gallium-67-labeled lactam bridge-cyclized α-melanocyte stimulating hormone peptide for primary and metastatic melanoma imaging. *Bioconjug. Chem.*, **2009**, *20*(12), 2356–2363.

[138] Guo, H.; Yang, J.; Gallazzi, F.; Prossnitz, E.R.; Sklar, L.A.; Miao, Y. Effect of DOTA position on melanoma targeting and pharmacokinetic properties of ^{111}In-labeled lactam bridge-cyclized α-melanocyte stimulating hormone peptide. *Bioconjug. Chem.*, **2009**, *20*(11), 2162–2168.

[139] Guo, H.; Yang, J.; Gallazzi, F.; Miao, Y. Reduction of the ring size of radiolabeled lactam bridge-cyclized α-MSH peptide, resulting in enhanced melanoma uptake. *J. Nucl. Med.*, **2010**, *51*(3), 418–426.

[140] Guo, H.; Yang, J.; Gallazzi, F.; Miao, Y. Effects of the amino acid linkers on the melanoma-targeting and pharmacokinetic properties of ^{111}In-labeled lactam bridge-cyclized α-MSH peptides. *J. Nucl. Med.*, **2011**, *52*(4), 608–616.

[141] Guo, H.; Gallazzi, F.; Miao, Y. Gallium-67-labeled lactam bridge-cyclized α-MSH peptides with enhanced melanoma uptake and reduced renal uptake. *Bioconjug. Chem.*, **2012**, *23*(6), 1341–1348.

[142] Guo, H.; Miao, Y. Cu-64-labeled lactam bridge-cyclized α-MSH peptides for PET imaging of melanoma. *Mol. Pharm.*, **2012**, *9*(8), 2322–2330.

[143] Guo, H.; Miao, Y. Melanoma targeting property of a Lu-177-labeled lactam bridge-cyclized α-MSH peptide. *Bioorg. Med. Chem. Lett.*, **2013**, *23*(8), 2319–2323.

[144] Martin, M.E.; O'Dorisio, M.S.; Leverich, W.M.; Kloepping, K.C.; Schultz, M.K. "Click" cyclized gallium-68 labeled peptides for molecular imaging and therapy:

Synthesis and preliminary in vitro and in vivo evaluation in a melanoma model system. *Recent Results Cancer Res.*, **2013**, *194*, 149–175.

[145] Morais, M.; Oliveira, B.L.; Correia, J.D.; Oliveira, M.C.; Jiménez, M.A.; Santos, I.; Raposinho, P.D. Influence of the bifunctional chelator on the pharmacokinetic properties of $^{99m}Tc(CO_3)$-labeled cyclic α-melanocyte stimulating hormone. *J. Med. Chem.*, **2013**, *56*(5), 1961–1973.

[146] Guo, H.; Gallazzi, F.; Miao, Y. Design and evaluation of new Tc-99m-labeled lactam bridge-cyclized α-MSH peptides for melanoma imaging. *Mol. Pharm.*, **2013**, *10*(4), 1400–1408.

[147] Guo, H.; Miao, Y. Introduction of an 8-aminooctanoic acid linker enhances uptake of ^{99m}Tc-labeled lactam bridge-cyclized α-MSH peptide in melanoma. *J. Nucl. Med.*, **2014**, *55*(12), 2057–2063.

[148] Liu, L.; Xu, J.; Yang, J.; Feng, C.; Miao, Y. Imaging human melanoma using a novel Tc-99m-labeled lactam bridge-cyclized α-MSH peptide. *Bioorg. Med. Chem. Lett.*, **2016**, *26*(19), 4724–4728.

[149] Capello, A.; Krenning, E.P.; Bernard, B.F.; Breeman, W.A.; van Hagen, M.P., de Jong, M. Increased cell death after therapy with an Arg-Gly-Asp-linked somatostatin analog. *J. Nucl. Med.*, **2004**, *45*(10), 1716–1720.

[150] Yang, J.; Guo, H.; Gallazzi, F.; Berwick, M.; Padilla, R.S.; Miao, Y. Evaluation of a novel Arg-Gly-Asp-conjugated α-melanocyte stimulating hormone hybrid peptide for potential melanoma therapy. *Bioconjug. Chem.*, **2009**, *20*(8), 1634–1642.

[151] Yang, J.; Guo, H.; Miao, Y. Technetium-99-m-labeled Arg-Gly-Asp-conjugated α-melanocyte stimulating hormone hybrid peptides for human melanoma imaging. *Nucl. Med. Biol.*, **2010**, *37*(8), 873–883.

[152] Yang, J.; Miao, Y. Substitution of Gly with Ala enhanced the melanoma uptake of technetium-99m-labeled Arg-Ala-Asp-conjugated α-melanocyte stimulating hormone peptide. *Bioorg. Med. Chem. Lett*., **2012**, *22*(4), 1541–1545.

[153] Flook, A.M.; Yang, J.; Miao, Y. Evaluation of new Tc-99m-labeled Arg-X-Asp-conjugated α-melanocyte stimulating hormone peptides for melanoma imaging. *Mol. Pharm.*, **2013**, *10*(9), 3417–3424.

[154] Yang, J.; Guo, H.; Padilla, R.S.; Berwick, M.; Miao,Y. Replacement of the Lys linker with an Arg linker resulting in improved melanoma uptake and reduced renal uptake of Tc-99m-labeled Arg-Gly-Asp-conjugated α-melanocyte stimulating hormone hybrid peptide. *Bioorg. Med. Chem.*, **2010**, *18*(18), 6695–6700.

[155] Yang, J.; Flook, A.M.; Feng, C.; Miao, Y. Linker modification reduced the renal uptake of technetium-99m-labeled Arg-Ala-Asp-conjugated α-melanocyte stimulating hormone peptide. *Bioorg. Med. Chem. Lett.*, **2014**, *24*(1), 195–198.

[156] Yang, J.; Lu, J.; Miao, Y. Structural modification on the Lys linker enhanced tumor to kidney uptake ratios of ^{99m}Tc-labeled RGD-conjugated α-MSH hybrid peptides. *Mol. Pharm.*, **2012**, *9*(5), 1418–1424.

[157] Flook, A.M.; Yang, J.; Miao, Y. Substitution of the Lys linker with the β-Ala linker dramatically decreased the renal uptake of ^{99m}Tc-labeled Arg-X-Asp-conjugated and X-Ala-Asp-conjugated α-melanocyte stimulating hormone peptides. *J. Med. Chem.*, **2014**, *57*(21), 9010–9018.

[158] Xu, J.; Yang, J.; Miao, Y. Dual receptor-targeting ^{99m}Tc-labeled Arg-Gly-Asp-conjugated α-melanocyte stimulating hormone hybrid peptides for human melanoma imaging. *Nucl. Med. Biol.*, **2015**, *42*(4), 369–374.

[159] Yang, J.; Hu, C.A.; Miao, Y. Tc-99m-labeled RGD-conjugated α-melanocyte stimulating hormone hybrid peptides with reduced renal uptake. *Amino Acids*, **2015**, *47*(4), 813–823.

[160] Miao, Y.; Quinn, T.P. Peptide-targeted radionuclide therapy for melanoma. *Crit. Rev. Oncol. Hematol.*, **2008**, *67*(3), 213–228.

[161] Eberle, A.N.; Bapst, J.P.; Calame, M.; Tanner, H.; Froidevaux, S. MSH radiopeptides for targeting melanoma metastases. *Adv. Exp. Med. Biol.*, **2010**, *681*, 133–142.

[162] Quinn, T.P.; Zhang, X.; Miao, Y. Targeted melanoma imaging and therapy with radiolabeled α-melanocyte stimulating hormone peptide analogues. *G. Ital. Dermatol. Venereol.*, **2010**, *145*(2), 245–258.

[163] Miao, Y.; Hoffman, T.J.; Quinn, T.P. Tumor-targeting properties of ^{90}Y- and ^{177}Lu-labeled α-melanocyte stimulating hormone peptide analogues in a murine melanoma model. *Nucl. Med. Biol.*, **2005**, *32*(5), 485–493.

[164] Miao, Y.; Fisher, D.R.; Quinn, T.P. Reducing renal uptake of ^{90}Y- and ^{177}Lu-labeled α-melanocyte stimulating hormone peptide analogues. *Nucl. Med. Biol.*, **2006**, *33*(6), 723–733.

[165] Miao, Y.; Shelton, T.; Quinn, T.P. Therapeutic efficacy of a ^{177}Lu-labeled DOTA conjugated α-melanocyte-stimulating hormone peptide in a murine melanoma-bearing mouse model. *Cancer Biother. Radiopharm.*, **2007**, *22*(3), 333–341.

[166] Miao, Y.; Owen, N.K.; Fisher, D.R.; Hoffman, T.J.; Quinn, T.P. Therapeutic efficacy of a ^{188}Re-labeled α-melanocyte-stimulating hormone peptide analog in murine and human melanoma-bearing mouse models. *J. Nucl. Med.*, **2005**, *46*(1), 121–129.

[167] Miao, Y.; Hylarides, M.; Fisher, D.R.; Shelton, T.; Moore, H.; Wester, D.W.; Fritzberg, A.R.; Winkelmann, C.T.; Hoffman, T.; Quinn, T.P. Melanoma therapy via peptide-targeted α-radiation. *Clin. Cancer Res.*, **2005**, *11*(15), 5616–5621.

[168] De Jong, M.; Breeman, W.A.P.; Kwekkeboom, D.J.; Valkema, R.; Krenning, E. Tumor imaging and therapy using radiolabeled somatostatin analogues. *Acc. Chem. Res.*, **2008**, *42*(7), 873–880.

[169] Cybulla, M.; Weiner, S.M.; Otte, A. Is 90Y-DOTATOC treatment for neuroendocrine tumours safe? *Med. Sci. Monit.*, **2002**, *8*(4), LE7.

[170] Mikolajczak, R.; Maecke, H.R. Radiopharmaceuticals for somatostatin receptor imaging. *Nucl. Med. Rev. Cent. East Eur.*, **2016**, *19*(2), 126–132.

[171] Newton, J.R.; Miao, Y.; Deutscher, S.L.; Quinn, T.P. Melanoma imaging with pretargeted bivalent bacteriophage. *J. Nucl. Med.*, **2007**, *48*(3), 429–436.

[172] Raposinho, P.D.; Correia, J.D.G.; Oliveira, M.C.; Santos, I. Melanocortin-1 receptor-targeting with radiolabeled cyclic α-melanocyte-stimulating hormone analogs for melanoma imaging. *Biopolymers*, **2010**, *94*(6), 820–829.

[173] Maaser, C.; Kannengiesser, K.; Kucharzik, T. Role of the melanocortin system in inflammation. *Ann. N.Y. Acad. Sci.*, **2006**, *1072*, 123–134.

[174] Patel, H.B.; Montero-Melendez, T.; Greco, K.V.; Perretti, M. Melanocortin receptors as novel effectors of macrophage responses in inflammation. *Front. Immunol.*, **2011**, *2.41*. DOI: 10.3389/fimmu.2011.00041

[175] Hoch, M.; Hirzel, E.; Lindinger, P.; Eberle, A.N.; Linscheid, P.; Martin, I.; Peters, T.; Peterli, R. Weak functional coupling of the melanocortin-1 receptor expressed in human adipocytes. *J. Recept. Signal Transduct.*, **2008**, *28*(5), 485–504.

[176] DeNardo, S.J.; Erickson, K.L.; Benjamini, E.; Hines, H.; Scibeinski, R. Radioimmunotherapy for melanoma. *Clin. Res.*, **1981**, *29*, 434–440.

[177] Larson, S.M.; Carrasquillo, J.A.; McGuffin, R.W.; Krohn, K.A.; Ferens, J.M.; Hill, L.D.; Beaumier, P.L.; Reynolds, J.C.; Hellström, K.E.; Hellström, I. Use of I-131 labeled, murine Fab against a high molecular weight antigen of human melanoma: preliminary experience. *Radiology*, **1985**, *155*(2), 487–492.

[178] Dadachova, E.; Casadevall, A. Renaissance of targeting molecules for melanoma. *Cancer Biother. Radiopharm.*, **2006**, *21*(6), 545–552.

[179] Rosas, A.L.; Nosanchuk, J.D.; Feldmesser, M.; Cox, G.M.; McDade, H.C.; Casadevall, A. Synthesis of polymerized melanin by *Cryptococcus neoformans* in infected rodents. *Infect. Immun.*, **2000**, *68*(5), 2845–2853.

[180] Dadachova, E.; Nosanchuk, J.D.; Shi, L.; Schweitzer, A.D.; Frenkel, A.; Nosanchuk, J.S.; Casadevall, A. Dead cells in melanoma tumors provide abundant antigen for targeted delivery of ionizing radiation by a mAb to melanin. *Proc. Natl. Acad. Sci. USA*, **2004**, *101*(41), 14865–14870.

[181] Klein, M.; Lotem, M.; Peretz, T.; Zwas, S.T.; Mizrachi, S.; Liberman, Y.; Chisin, R.; Schachter, J.; Ron, I.G.; Iosilevsky, G.; Kennedy, J.A.; Revskaya, E.; de Kater, A.W.; Banaga, E.; Klutzaritz, V.; Friedmann, N.; Galun, E.; DeNardo, G.L.; De Nardo, S.J.; Casadevall, A.; Dadachova, E.; Thornton, G.B. Safety and efficacy of 188-rhenium-labeled antibody to melanin in patients with metastatic melanoma. *J. Skin Cancer*, **2013**, *2013*, 828329. DOI: 10.1155/2013/828329

[182] Dadachova, E.; Moadel, T.; Schweitzer, A.D.; Bryan, R.A.; Zhang, T.; Mints, L.; Revskaya, E.; Huang, X.; Ortiz, G.; Nosanchuk, J.S.; Nosanchuk, J.D.; Casadevall, A. Radiolabeled melanin-binding peptides are safe and effective in treatment of human pigmented melanoma in a mouse model of disease. *Cancer Biother. Radiopharm.*, **2006**, *21*(2), 117–129.

[183] Howell, R.C.; Revskaya, E.; Pazo, V.; Nosanchuk, J.D.; Casadevall, A.; Dadachova, E. Phage display library derived peptides that bind to human tumor melanin as potential vehicles for targeted radionuclide therapy of metastatic melanoma. *Bioconjug. Chem.*, **2007**, *18*(6), 1739–1748.

[184] Joyal, J.L.; Barrett, J.A.; Marquis, J.C.; Chen, J.; Hillier, S.M.; Maresca, K.P.; Boyd, M.; Gage, K.; Nimmagadda, S.; Kronauge, J.F.; Friebe, M.; Dinkelborg, L.; Stubbs, J.B.; Stabin, M.G.; Mairs, R.; Pomper, M.G.; Babich, J.W. Preclinical evaluation of an ^{131}I-labeled benzamide for targeted radiotherapy of metastatic melanoma. *Cancer Res.*, **2010**, *70*(10), 4045–4053.

[185] Mier, W.; Kratochwil, C.; Hassel, J.C.; Giesel, F.L.; Beijer, B.; Babich, J.W.; Friebe, M.; Eisenhut, M.; Enk, A.; Haberkorn U. Radiopharmaceutical therapy of patients with metastasized melanoma with the melanin-binding benzamide ^{131}I-BA52. *J. Nucl. Med.*, **2014**, *55*(1), 9–14.

[186] Dolmans, D.E.; Fukumura, D.; Jain, R.K. Photodynamic therapy for cancer. *Nat. Rev. Cancer*, **2003**, *3*(5), 380–387.

[187] Wilson, B.C.; Patterson, M.S.; Lilge, L. Implicit and explicit dosimetry in photodynamic therapy: a new paradigm. *Lasers Med. Sci.*, **1997**, *12*(3), 182–199.

[188] Mustafa F, Jaafar M. Comparison of wavelength-dependent penetration depths of lasers in different types of skin in photodynamic therapy. *Indian J Phys.* **2013**, *87*(3), 203–209.

[189] Rout, B. A miniaturized therapeutic chromophore for multiple metal pollutant sensing, pathological metal diagnosis and logical computing. *Sci. Rep.*, **2016**, *6*, 27115. DOI: 10.1038/srep27115.

[190] Rout, B.; Bigliardi, P. Pattern-generating unimolecular sensors: For future differential sensing and molecular computing. *Synlett*, **2017**, *28*, A-E. DOI: 10.1055/s-0036-1588721

[191] Nakayama, T.; Otsuka, S.; Kobayashi, T.; Okajima, H.; Matsumoto, K.; Hagiya, Y.; Inoue, K.; Shuin, T.; Nakajima, M.; Tanaka, T., Ogura, S.-I. Dormant cancer cells accumulate high protoporphyrin IX levels and are sensitive to 5-aminolevulinic acid-based photodynamic therapy. *Sci. Rep.*, **2016**, *6*, 36478. DOI: 10.1038/srep3

[192] Slastnikova, T.A.; Rosenkranz, A.A.; Lupanova, T.N.; Gulak, P.V.; Gnuchev, N.V.; Sobolev, A.S. Study of efficiency of the modular nanotransporter for targeted delivery of photosensitizers to melanoma cell nuclei in vivo. *Dokl. Biochem. Biophys*., **2012**, *446*, 235–237.

FIGURE LEGENDS

Fig. (1). Peptides for skin cancer management. Peptides serve a multitude of functions, e.g. as growth inhibitors, as vehicle for cancer localization and treatment (radiopeptides, photosensitizer-peptide conjugates), as lead compounds for the development of non-peptide small-molecule inhibitors or as antigens for the generation of monoclonal antibodies against antigens in cancer cells.

Fig. (2). Principle of peptide-receptor radiotherapy (PRRT) of melanoma with MSH peptides. The radiolabeled peptide is injected i.v. and is accumulated in MC1R-expressing melanoma tumors through internalization by the cells. Depending on the purpose of the radiopeptide, either therapeutic Auger-, α- or β-emitting radiometal ions, or diagnostic γ-emitting metal ions are inserted into the chelator-conjugated peptide. Alternatively, positron-emitting ^{18}F-, ^{64}Cu- or ^{68}Ga-containing MSH radiopeptides are applied for PET (not shown).

Fig. (3). Time-course of the uptake of [^{111}In]DOTA-Phospho-MSH$_{2-9}$ (**L14**) by mouse B16-F1 melanoma cells *in vitro* and release of ^{111}In from the cells in the absence of radioligand. (A) B16-F1 cells seeded in 6-well plates were exposed to 74 kBq of **L14** and incubated for 0.5, 2 and 3.5 h. Total radioactivity bound to the cells consisted of surface bound and internalized radiopeptide. The former was determined by a dissociation step (details see [117]). (B) Retention of internalized radioactivity by the cells kept in normal medium at 37°C for 1, 2 and 4.5 h.

Fig. (4). Chemical structures of (A) DOTA-NAP-amide (**L9**), (B) DOTA-Gal-NAP-amide (**L12**) and (C) DOTA-Phospho-MSH$_{2-9}$ (**L14**).

Fig. (5). Induced intracutaneous mouse B16-F1 melanoma (A) and the corresponding autoradiogram (B) 4 h after *in vivo* injection of [^{111}In]DOTA-β-Ala-Nle-Asp-His-*D*-Phe-Arg-Trp-Lys-NH$_2$ (**L8**) into experimental animals. The tissue was collected and immediately fixed, frozen, dried in a desiccator, exposed to a storage phosphor plate (for B) and finally scanned (for A), as described in detail in [110]. Equivalent results were obtained with [^{111}In]DOTA-NAP-amide (**L9**) [79].

Fig. (6). Metastatic melanotic melanoma in the lung (A), amelanotic lung melanoma (C) and melanotic liver melanoma metastases (E), and the corresponding autoradiograms (B, D, F). Experimental conditions as in Fig. **5** using either **L8** or **L9** (see also [79, 110]).

Fig. (7). Tumor-to-kidney ratios of ^{111}In-labeled DOTA-NAP-amide analogs with net charges between −2 and +2 at observation time intervals of 4 h, 24 h, and 48 h after injection in tumor-bearing mice. *Net charge -2:* {[Ac-Nle^4,Asp^5,*D*-Phe^7,Lys^{11}(DOTA)]-α-MSH$_{4-11}$}-*D*-Asp-*D*-Asp-OH; *net charge -1:* [DOTA-Gly^2,Tyr(P)^3,Nle^4,Asp^5,*D*-Phe^7]-α-MSH$_{2-9}$; *net charge 0:* [Ac-Nle^4,Asp^5,*D*-Phe^7,Lys^{11}(DOTA)]-α-MSH$_{4-11}$-carboxylate; *net charge +1:* [Ac-Nle^4,Asp^5,*D*-Phe^7,Lys^{11}(DOTA)]-α-MSH$_{4-11}$; *net charge +2:* [DOTA-Nle^4,Asp^5,*D*-Phe^7]-α-MSH$_{4-11}$. The bars represent the mean of 6−12 determinations ± SEM; the values originate from references [79, 114, 117] where experimental details can be found.

Fig. (8). Chemical structure of (A) Re-cyclized (Ala-triazol)Ac-Re[Arg^{11}]CCMSH (**C3a**) and lactam-bridge-cyclized Pz^4-β-Ala-Nle-*cyclo*[Asp-His-*D*-Phe-Arg-Trp-Lys-NH$_2$] (**C10**).

Fig. (9). Tumor imaging with ([^{99m}Tc(CO)$_3$]Ala-triazol)Ac-Re[Arg^{11}]CCMSH (**C3a**) in B16/F1 melanoma bearing C57 mice 2 h post injection (reproduced from [104]). Whole body and transaxial SPECT images of **C3a** (A, B) or transaxial and whole body images of **C3a** in the presence of the unlabeled NDP-MSH (C, D) as part of a blocking study. Tumor-bearing mice were injected with 18.5 MBq of **C3a** for SPECT imaging studies. Tumor uptake specificity of **C3a** was determined by co-injecting 20 μg of unlabeled NDP-MSH at 2 h post-injection. (Figure kindly provided by Professor T.P. Quinn, University of Missouri, Columbia, MO and reproduced with permission.)

Fig. (10). Schematic representation of principle of targeted photodynamic therapy in skin. *Left:* Cellular uptake of peptide with attached photosensitizer (yellow star) by the skin. *Right:* Cellular necrosis induced by ROS (red dot) after exposure of photosensitizer to different wavelengths of light (UV or IR) that penetrate the skin to different depths.

Fig. (11). (A) Chemical structure of HPPH-NAP-amide. (B) Melanin production by B16-F10 cells treated with α-MSH (10 nM), NAP-amide (1 μM) and HPPH-NAP-amide (1 μM); optical density (OD) of melanin was measured at 475 nm after 72 h. (C) Cell proliferation curves of B16-F10 cells kept in the dark and treated with 10 μM or 1 μM HPPH-NAP-amide compared to controls.

Table 1. Amino acid sequence of lead peptides for PRRT and MPRT of melanoma and for the treatment of melanotic lesions

Peptide	Biological role	Application
α-MSH: Ac-Ser-Tyr-Ser-Met-Glu-His-Phe-Arg-Trp-Gly-Lys-Pro-Val-NH_2	Stimulation of melanogenesis	Melanoma targeting (PRRT) *(early experiments)*
NDP-MSH: Ac-Ser-Tyr-Ser-Nle-Glu-His-*D*-Phe-Arg-Trp-Gly-Lys-Pro-Val-NH_2 and numerous analogs and fragments, e.g.: *cap*-His-*D*-Phe-Arg-Trp-*cap*	Stimulation of melanogenesis	Melanoma targeting (PRRT) Cosmetic tanning
NAP: Ac-Nle-Asp-His-*D*-Phe-Arg-Trp-Gly-Lys-NH_2	Stimulation of melanogenesis	Melanoma targeting (PRRT)
Cyclic γ-MSH analog: cyclo-[$(CH_2)_3$CO-Gly-His-*D*-Phe-Arg-*D*-Trp-Cys(S-)]- -Asp-Arg-Phe-Gly-NH_2	Inhibition of melanogenesis *(ASIP-like backbone structure)*	Potentially useful for melanoma targeting
MBP: Tyr-Gly-Arg-Lys-Phe-Trp-His-Gly-Arg-His (4B4) Asn-Pro-Asn-Trp-Gly-Pro-Arg	Melanin binding peptides	Melanoma targeting (MPRT)
Decapeptide-12: Tyr-Arg-Ser-Arg-Lys-Tyr-Ser-Ser-Trp-Tyr	Inhibition of melanogenesis *(inhibition of tyrosinase)*	Melasma treatment Lentigo treatment
Photosensitizer-NAP: HPPH-Nle-Asp-His-*D*-Phe-Arg-Trp-Gly-Lys-NH_2	Stimulation of melanogenesis *(in the dark)*; cell arrest/killing *(when exposed to LED light)*	Melasma treatment Melanoma treatment

Table 2. Sequence of selected linear MSH radiopeptides and their biological characteristics.

MSH peptide–chelator complex		Nuclide	Characteristics	Reference
L1	DTPA-*bis*MSH (= DTPA{[-NH-Ser^{1}]-α-MSH}$_2$)	^{111}In	89% of melanoma lesions in patients detected; high kidney and liver uptake	71, 73
L2	DTPA-Nle-Asp-His-*D*-Phe-Arg-Trp-Lys-NH_2	^{111}In	5x higher tumor uptake in mice as compared to DTPA-*bis*MSH	72
L3	DTPA-Nle-Asp-His-*D*-Phe-Arg-Trp-Lys(*bis*DHP)-NH_2	^{111}In	Good tumor uptake in mice; high kidney uptake; moderate liver uptake; best of three similar analogs	74
L4	DTPA-*bis*{Nle-Asp-His-*D*-Phe-Arg-Trp-Lys-NH_2}	^{111}In	Moderate tumor uptake; very high kidney and liver uptake; best of three similar dimeric analogs	74
L5	DTPA-*bis*{NDP-MSH}	^{111}In	Good tumor uptake; high kidney and liver uptake	109
L6	DTPA-NDP-MSH	^{111}In	Good tumor uptake; relative high kidney an thyroid uptake; no liver uptake	109
L7	DOTA-NDP-MSH	^{111}In	Good tumor uptake; kidney uptake and moderate uptake by bone marrow and skin; low liver uptake	110
L8	DOTA-βAla-Nle-Asp-His-*D*-Phe-Arg-Trp-Lys-NH_2	^{111}In	Precise localization of metastatic tumor lesions; low non-specific uptake, except kidneys	110
L9	Ac-Nle-Asp-His-*D*-Phe-Arg-Trp-Gly-Lys(DOTA)-NH_2	^{111}In, $^{67/68}$Ga, ^{90}Y	Excellent localization of metastatic tumor lesions with ^{67}Ga; precise tumor localization with ^{68}Ga by PET; good tumor uptake and low non-specific uptake, except kidneys	79
L10	Ac-Nle-Asp-His-*D*-Phe-Arg-Trp-Gly-Lys(SFB)-NH_2	^{18}F	Similar in vitro data as with DOTA-NAP-amide; moderate tumor localization with PET	112, 113
L11	DOTA-{*di*-[Nle-Asp-His-*D*-Phe-Arg-Trp]} analogs	^{111}In	Three different dimerized MSH_{4-9} peptides containing DOTA showed higher MC1R affinity but lower tumor uptake and higher kidney and liver uptake	115
L12	Gal-Nle-Asp-His-*D*-Phe-Arg-Trp-Gly-Lys(DOTA)-NH_2	^{111}In	20% improvement of tumor-to-kidney ratios compared to DOTA-NAP-amide; best of five other glycopeptides	116
L13	DOTA-Nle-Asp-His-*D*-Phe-Arg-Trp-Gly-Lys(Ac)-NH_2	^{111}In	Almost equivalent to DOTA-NAP-amide above; best of six similar compounds	114
L14	DOTA-Gly-Tyr(OPO_3H_2)-Nle-Asp-His-*D*-Phe-Arg-Trp-NH_2	^{111}In	Similar tumor uptake as with DOTA-NAP-amide but 44% lower kidney uptake	117
L15	NOTA-Bz-NCS-Ahx-βAla-Nle-Aps-His-*D*-Phe-Arg-Trp-Gly-NH_2	^{64}Cu	High MC1R binding affinity and good *in vivo* stability	99

Table 3. Sequence of selected cyclic MSH radiopeptides and their biological characteristics.

No.	MSH peptide–chelator complex	Nuclide	Characteristics	Reference
C1	Ac-Cys-Cys-Glu-His-*D*-Phe-Arg-Trp-Cys-Lys-Pro-Val-NH_2 ReO *(ReCCMSH)*	^{99m}Tc ^{188}Re	High MC1R affinity (IC_{50} 2.6 nM), comparable to linear peptides; good tumor localization with ^{99m}Tc	101
C2	Ac-Cys-Cys-Glu-His-*D*-Phe-Arg-Trp-Cys-Arg-Pro-Val-NH_2 ReO *(Re[Arg^{11}]CCMSH)*	^{188}Re ^{99m}Tc	High MC1R affinity (IC_{50} 1.9 nM), very good tumor uptake; kidney uptake lower than tumor uptake	123
C3a,b	(Ala-triazol)-Ac-Re[Arg^{11}]CCMSH, N_4-CO-Re[Arg^{11}]CCMSH	^{99m}Tc	High MC1R affinity (IC_{50} ~1 nM (**a**) and 2.4 nM (**b**)); good tumor localization; kidney uptake	104
C4	DOTA-Cys-Cys-Glu-His-*D*-Phe-Arg-Trp-Cys-Lys-Pro-Val-NH_2 ReO *(DOTA-ReCCMSH)*	^{111}In	High MC1R affinity (IC_{50} 1.2 nM); good tumor localization; kidney uptake similar to tumor uptake	126, 128
C5	DOTA-Cys-Cys-Glu-His-*D*-Phe-Arg-Trp-Cys-Arg-Pro-Val-NH_2 ReO *(DOTA-Re[Arg^{11}]CCMSH)*	^{111}In ^{64}Cu, ^{86}Y	High MC1R affinity (IC_{50} 1.2 nM); good tumor localization; kidney uptake lower than tumor uptake	128, 129
C6	CBTE2A-Cys-Cys-Glu-His-*D*-Phe-Arg-Trp-Cys-Arg-Pro-Val-NH_2 ReO	^{64}Cu	MC1R affinity 4–5x lower (IC_{50} 5.4 nM); good stability and good tumor localization; moderate kidney uptake	97
C7	DOTA-Nle-*cyclo*[Asp-His-*D*-Phe-Arg-Trp-Lys-NH_2]	^{111}In	High MC1R affinity (IC_{50} 1.2 nM); good tumor localization; kidney uptake slightly higher than for **C5**	139
C8	DOTA-Gly-Gly-Nle-*cyclo*[Asp-His-*D*-Phe-Arg-Trp-Lys-NH_2]	^{111}In, ^{177}Lu	High MC1R affinity (IC_{50} 2.1 nM); good tumor localization; kidney uptake markedly lower	140, 143
C9	NOTA-Gly-Gly-Nle-*cyclo*[Asp-His-*D*-Phe-Arg-Trp-Lys-NH_2]	^{67}Ga ^{64}Cu	High MC1R affinity (IC_{50} 1.6 nM); good tumor localization; further reduction of kidney uptake	141, 142
C10	DOTA-Gly-Gly-Nle-*cyclo*[Pra-His-*D*-Phe-Arg-Trp-Lys(N_3)-NH_2]	^{68}Ga	Triazol cyclized ClickMTII analog; IC_{50} 2.7 nM; good stability; tumor uptake 3.4x higher than kidney uptake; clear PET image	144
C11	Pz^4-β-Ala-Nle-*cyclo*[Asp-His-*D*-Phe-Arg-Trp-Lys-NH_2]	^{99m}Tc	High MC1R affinity (IC_{50} 0.16 nM); good stability and tumor localization; excellent tumor-to-kidney ratios	145
C12	HYNIC-Aoc-Nle-*cyclo*[Asp-His-*D*-Phe-Arg-Trp-Lys-NH_2]	^{99m}Tc	High MC1R affinity (IC_{50} 0.4 nM); good stability and tumor localization; excellent tumor-to-kidney ratios	147
C13	*cyclo*[Arg-Ala-Asp-*D*-Tyr-Asp]-β-Ala-Re[Arg^{11}]CCMSH	^{99m}Tc	Dual targeting peptide with modified RGD motif; high MC1R affinity (IC_{50} 0.35 nM); tumor uptake ~ kidney uptake	157

Figure 1

Peptides for skin cancer management

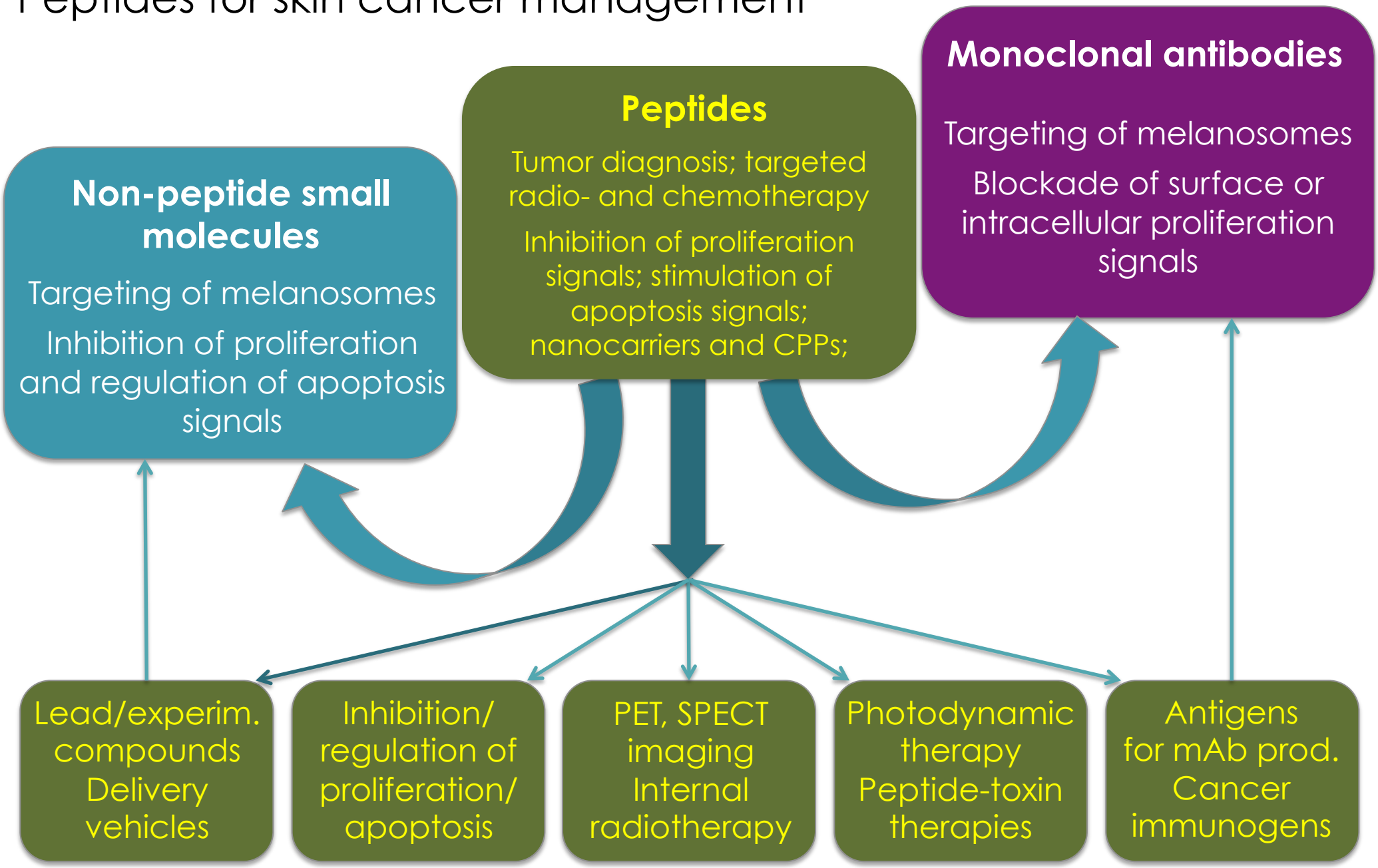

Melanoma PRRT with peptides

Figure 2

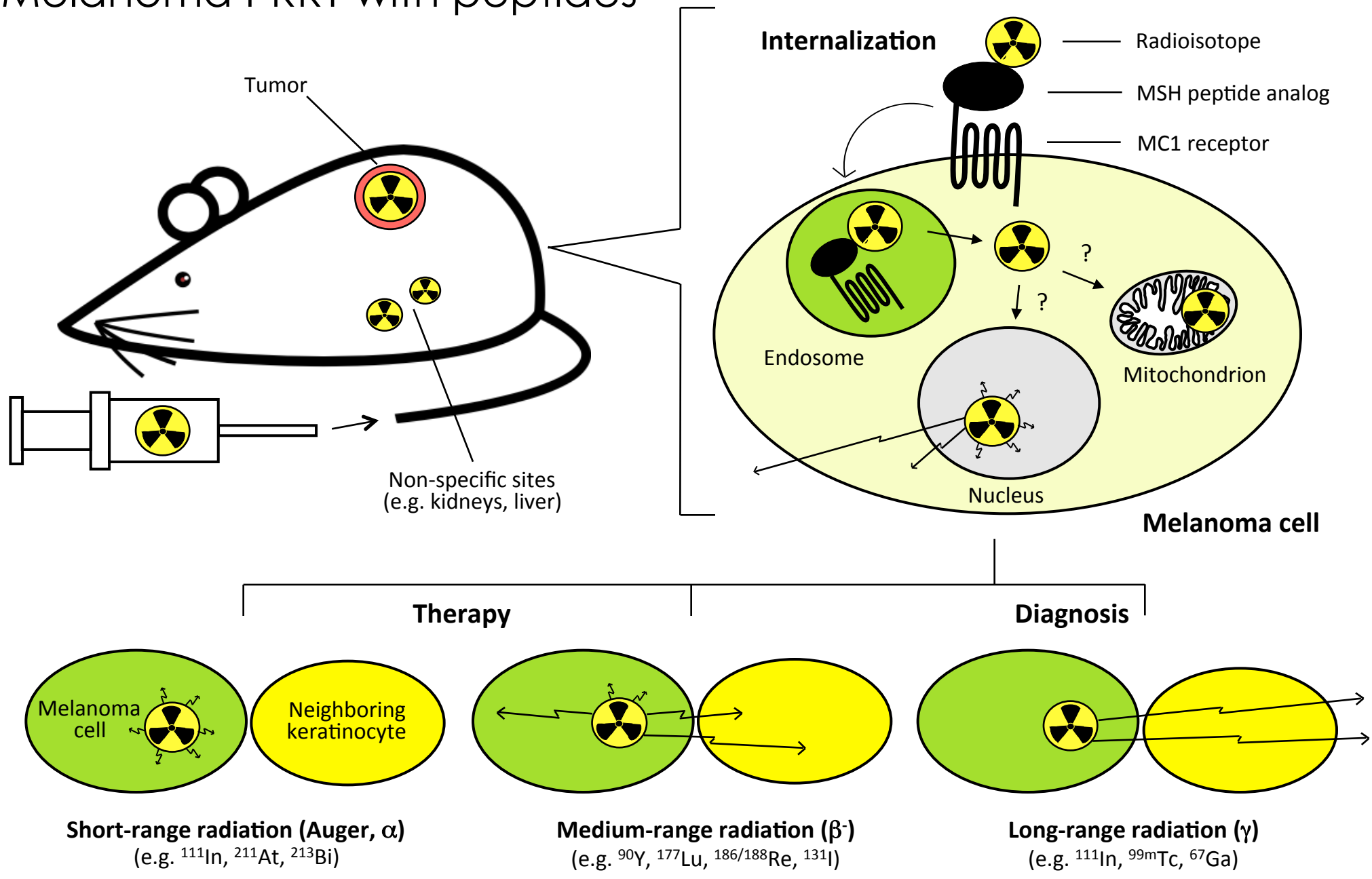

Figure 3

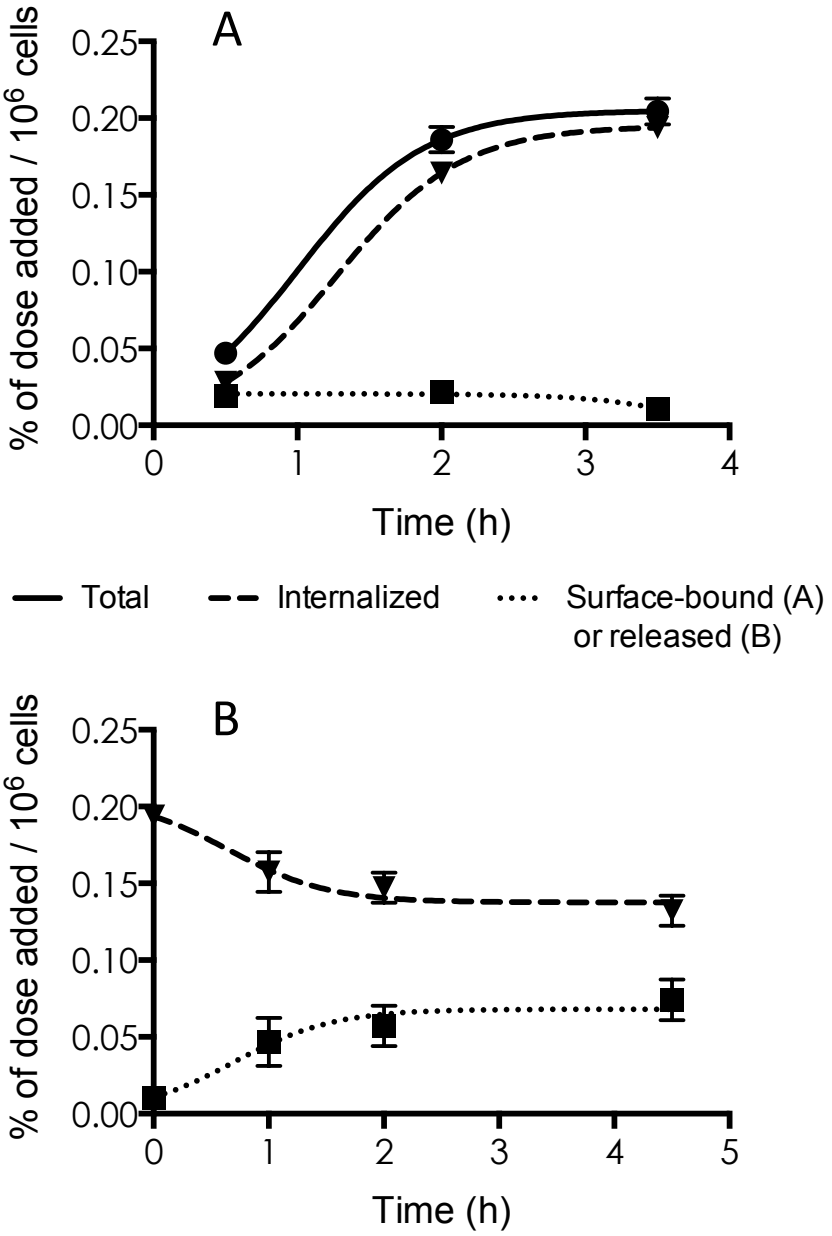
A
% of dose added / 10^6 cells
0.25
0.20
0.15
0.10
0.05
0.00
0
1
2
3
4
Time (h)
Total
Internalized
Surface-bound (A)
or released (B)
B
% of dose added / 10^6 cells
0.25
0.20
0.15
0.10
0.05
0.00
0
1
2
3
4
5
Time (h)

Figure 4

A DOTA-NAP-amide **L9**

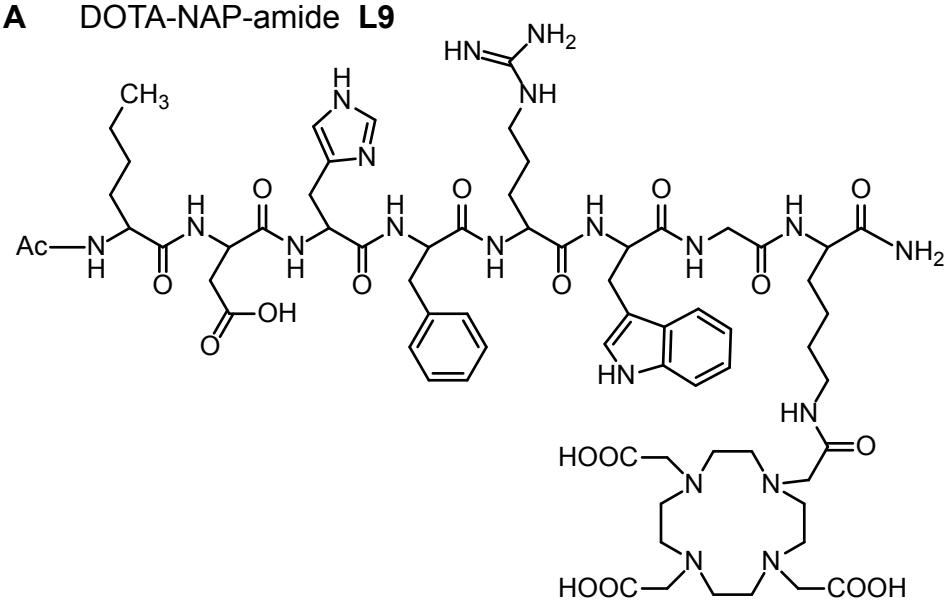

B DOTA-Gal-NAP-amide **L12**

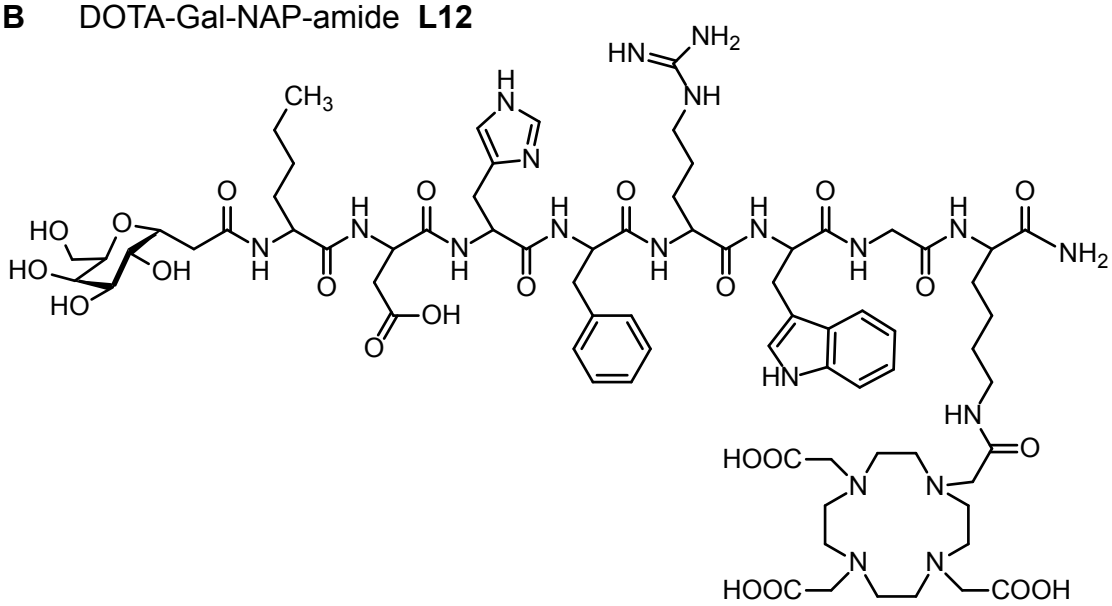

C DOTA-Phospho-MSH_{2-9} **L14**

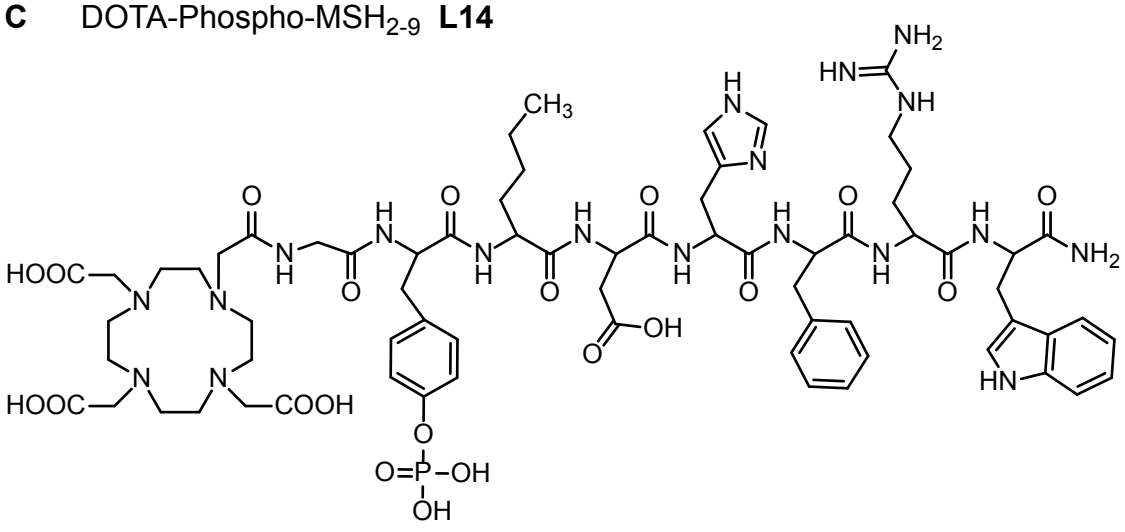

Figure 5

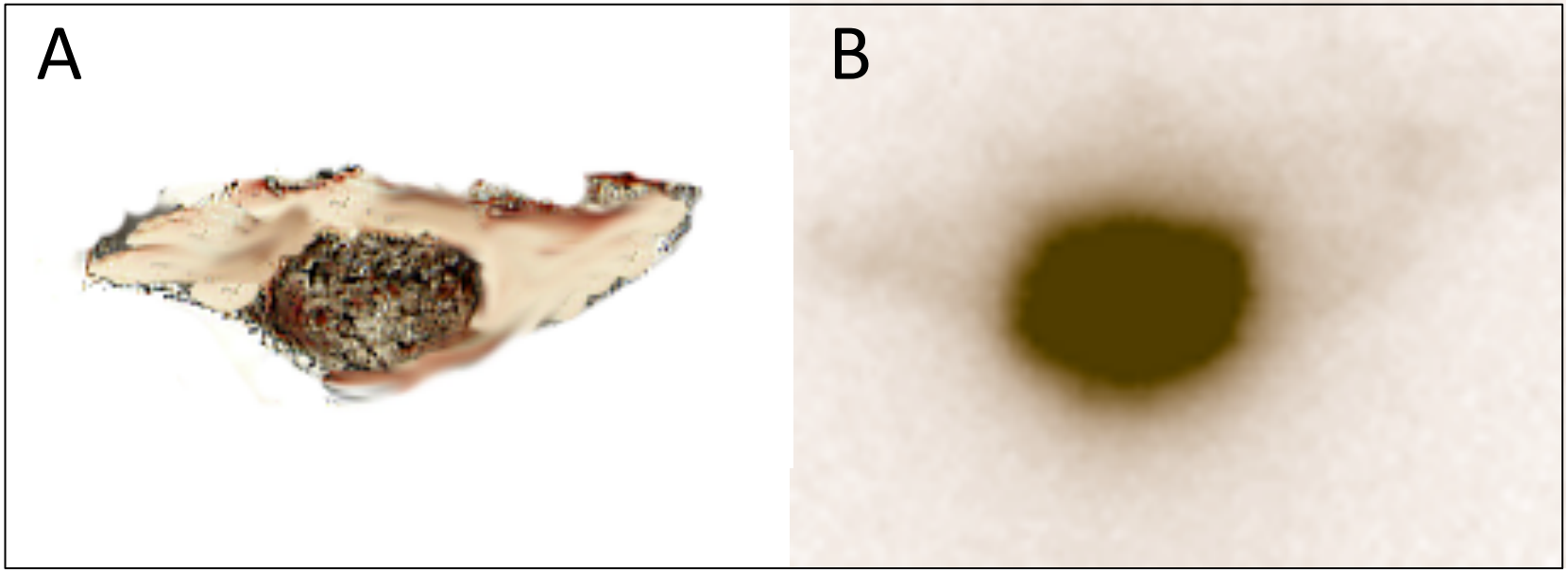

Figure 6

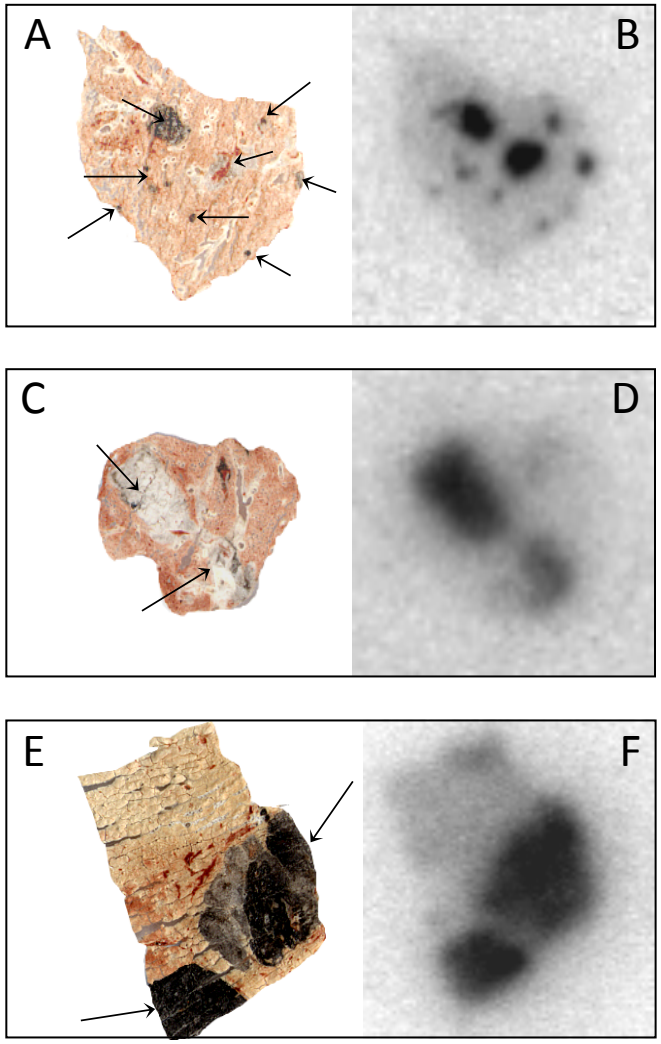

Figure 7

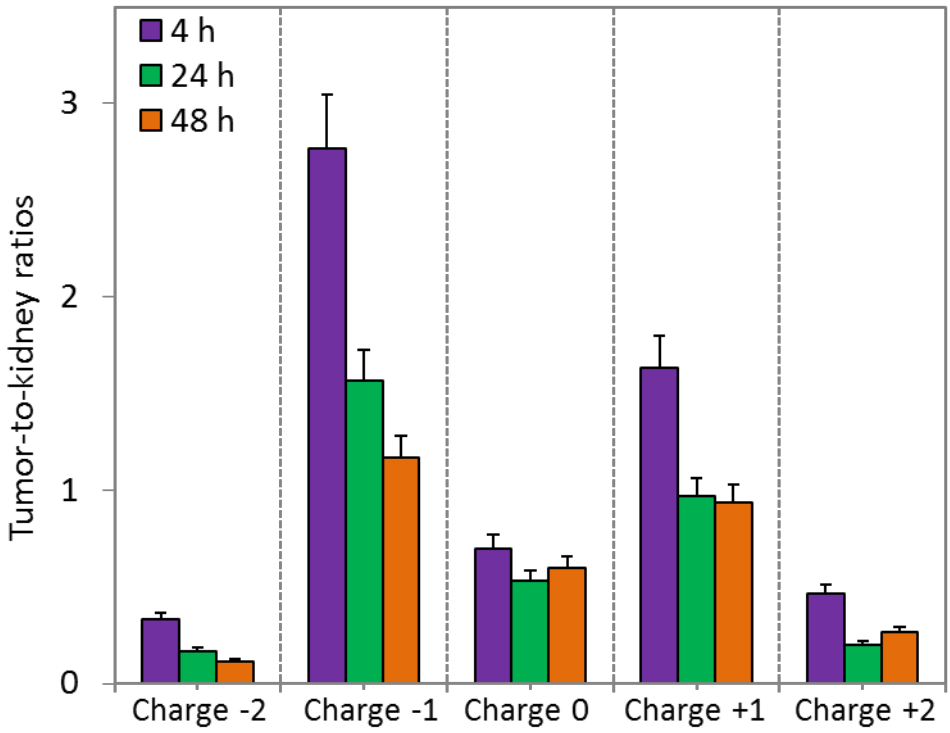
4 h
24 h
48 h
Tumor-to-kidney ratios
0
1
2
3
Charge -2
Charge -1
Charge 0
Charge +1
Charge +2

Figure 8

A (Ala-Triazol)Ac-Re[Arg^{11}]CCMSH **C3a**

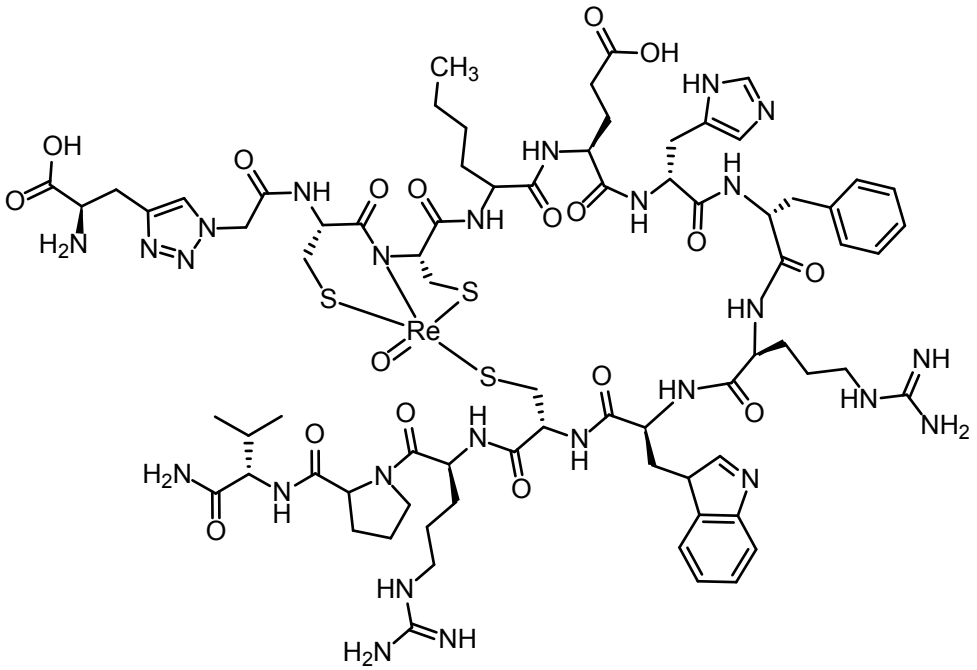

B Pz^{4}-β-Ala-Nle-*cyclo*[Asp-His-*D*-Phe-Arg-Trp-Lys-NH_2] **C10**

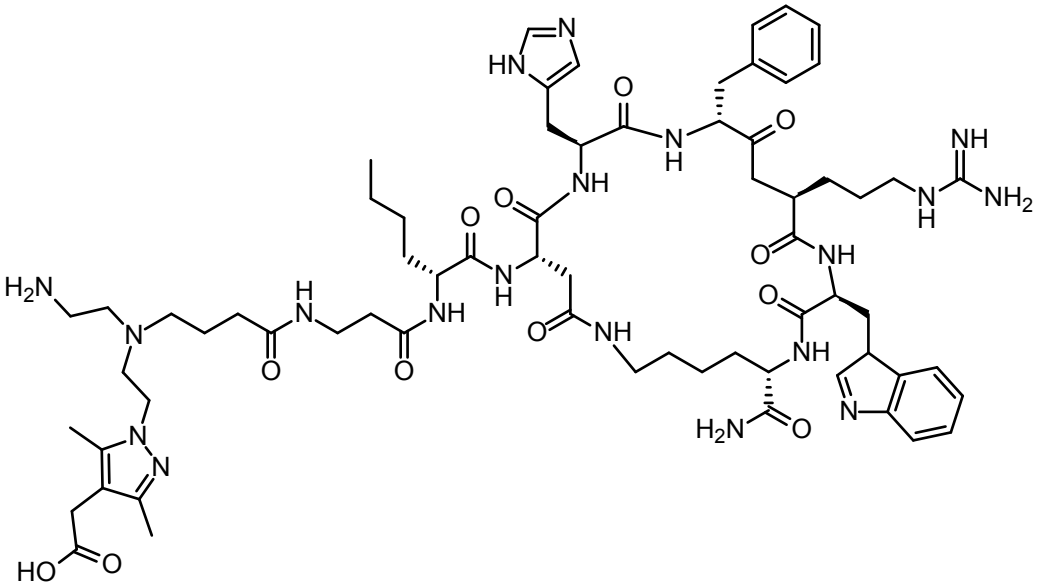

Figure 9

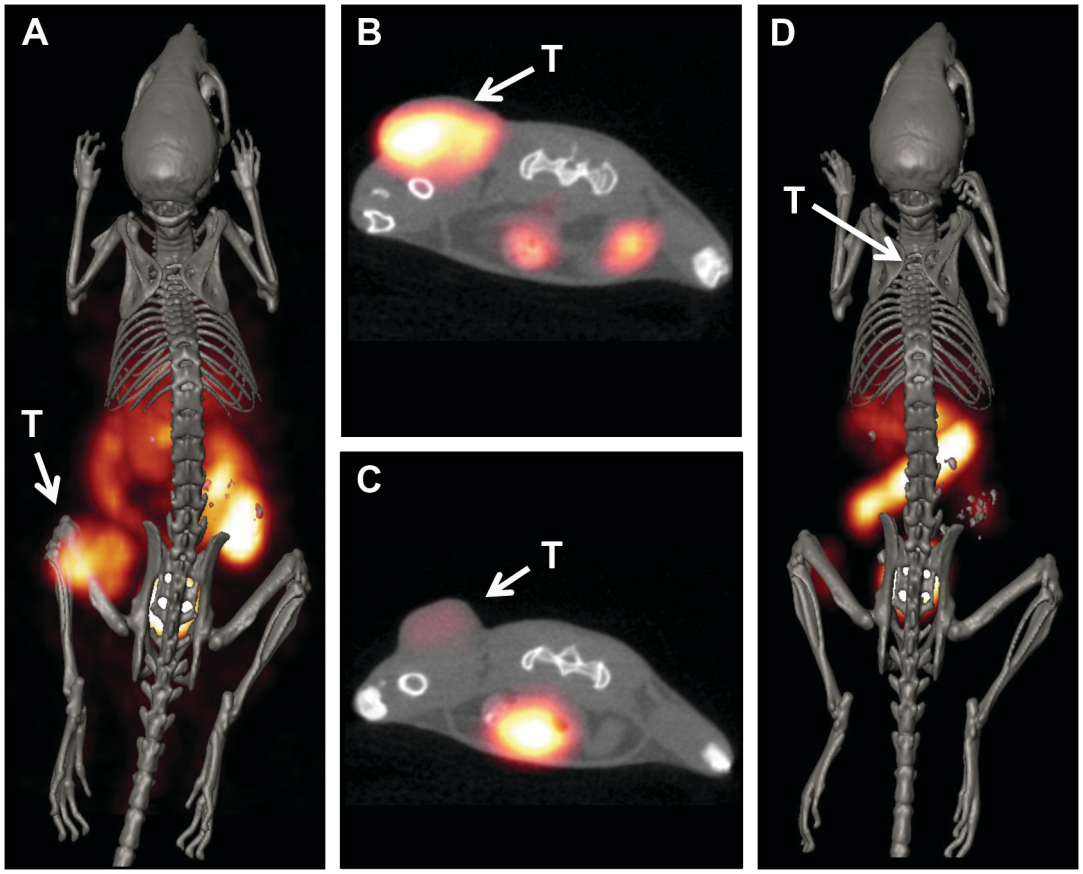

Figure 10

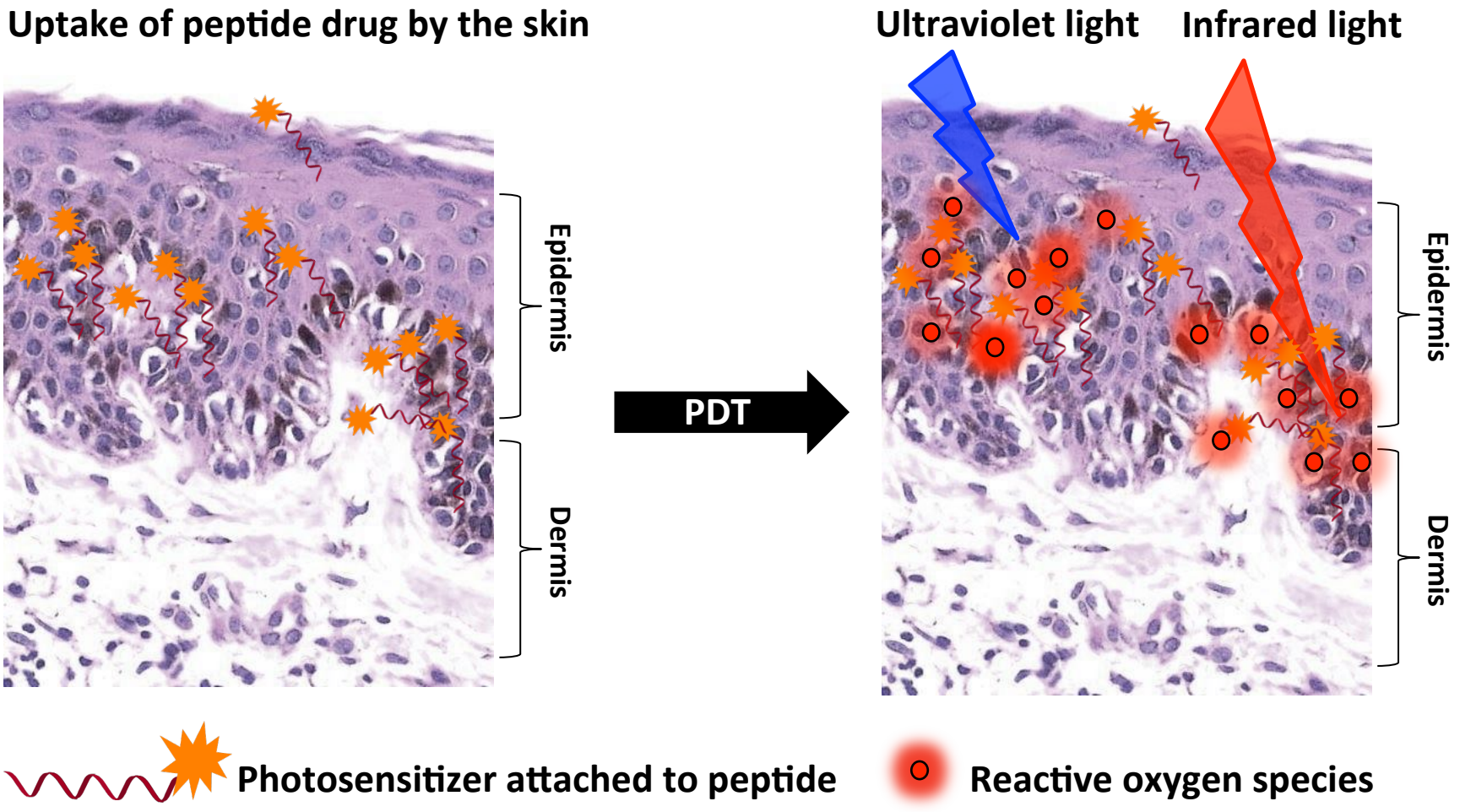
Uptake of peptide drug by the skin
Epidermis
Dermis
PDT
Ultraviolet light
Infrared light
Epidermis
Dermis
Photosensitizer attached to peptide
Reactive oxygen species

Figure 11

A

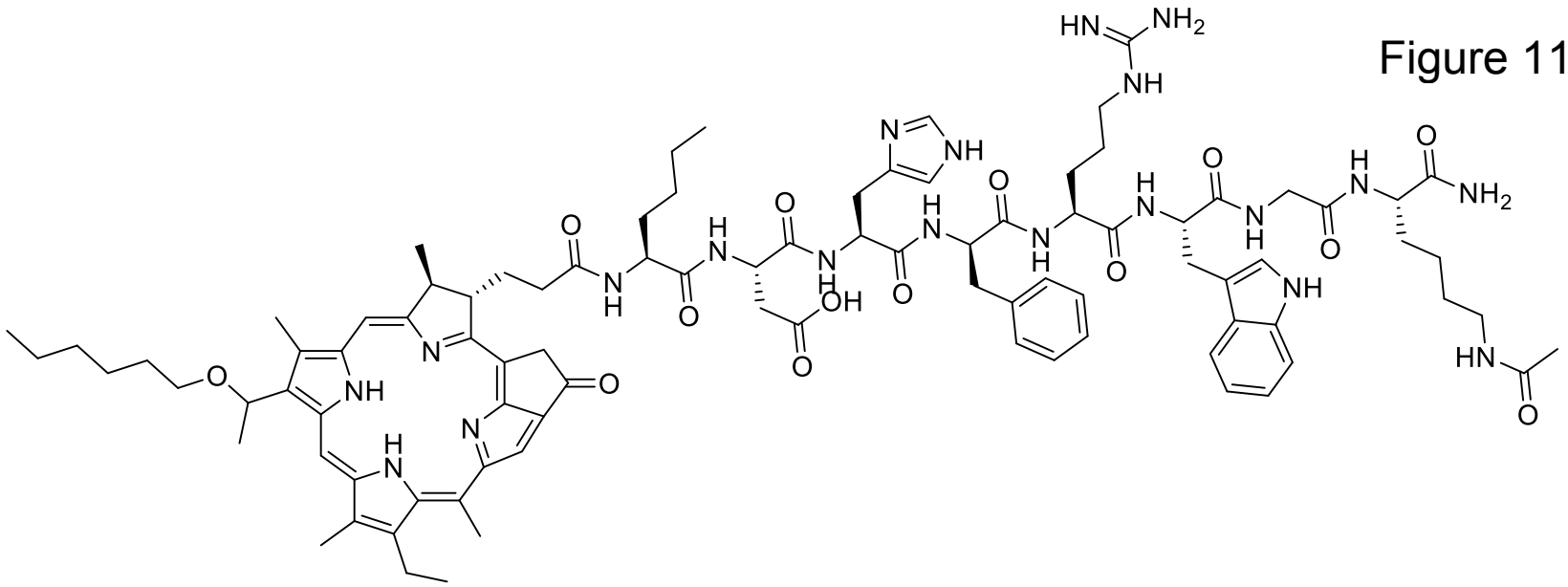

B

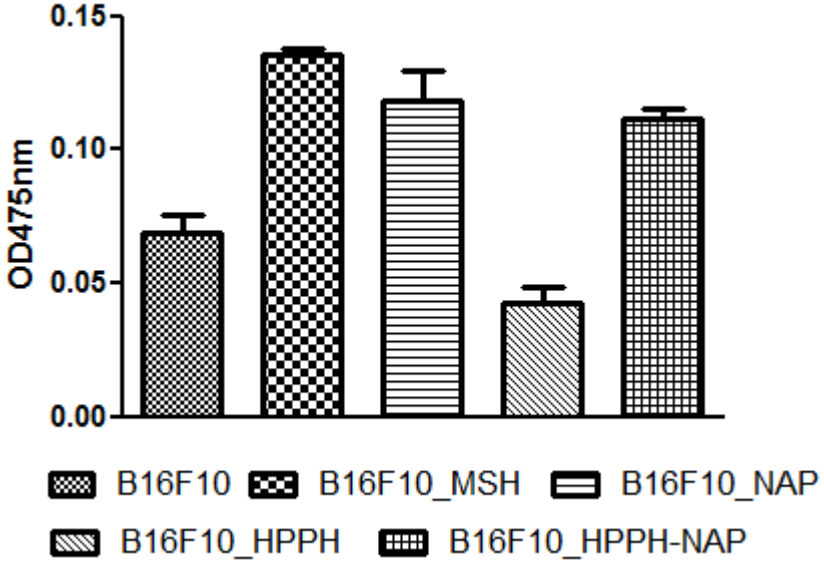

C